National Research Centre **“Kurchatov Institute”**

A.A. Logunov INSTITUTE FOR HIGH ENERGY PHYSICS
of the National Research Centre “Kurchatov Institute”

Single-spin physics in the SPD NICA project

V.V. Abramov, IHEP, Protvino

WORKSHOP:
Physics programme for the first stage of the NICA SPD experiment

Dubna, Russia, October 5, 2020

Talk content

1. Introduction
2. The Chromo-magnetic polarization of quarks (CPQ) model
3. Single-spin asymmetry (A_N) of hadron production
4. Hyperon polarization (P_N)
5. Conclusions

Introduction

Possible physics of single-spin processes in the SPD NICA project is proposed. This includes single-spin asymmetry (A_N) and hyperon transverse polarization (P_N) measurements in various types of collisions, including p+p, p+d, d+d, C+C and Ca+Ca collisions. The polarized p- and d-beams in the NICA collider can be used to study A_N for more than several dozen reactions at different energies in the energy range $3.4 < \sqrt{s} < 27$ GeV.

A number of interesting phenomena have been predicted for some reactions, such as the oscillation for $A_N(x_F)$ and $P_N(x_F)$, the resonance type dependence on the energy $\sqrt{s}$ for A_N and P_N, and the threshold dependence of A_N on the c.m. production angle. The dependence of A_N and P_N on event multiplicity is a new interesting phenomenon, which can be studied. The role of quark composition of particles involved in the reaction and color factor are discussed.

Single-spin asymmetry

Table 1 presents 27 inclusive reactions for which there are already data on the single-spin asymmetry of hadrons. For many of these reactions, the data are very limited in accuracy and kinematic area investigated. The first 14 reactions from the Table 1 can potentially be studied at the NICA collider using the SPD facility.

The initial state can be any with a polarized beam: p↑p, p↑d, d↑p, d↑d.

Table 1. Inclusive reactions for which the spin-spin asymmetry A_N was measured.

№	Reaction	№	Reaction	№	Reaction	№	Reaction
1	$p^\uparrow p(A) \to \pi^+ X$	8	$p^\uparrow p(A) \to pX$	15	$\bar{p}^\uparrow p \to \pi^+ X$	22	$\pi^- p^\uparrow \to \pi^0 X$
2	$p^\uparrow p(A) \to \pi^- X$	9	$p^\uparrow p(A) \to \bar{p}X$	16	$\bar{p}^\uparrow p \to \pi^- X$	23	$\pi^- d^\uparrow \to \pi^0 X$
3	$p^\uparrow p \to \pi^0 X$	10	$p^\uparrow p(A) \to J/\psi X$	17	$\bar{p}^\uparrow p \to \pi^0 X$	24	$K^- d^\uparrow \to \pi^0 X$
4	$p^\uparrow p(A) \to K^+ X$	11	$p^\uparrow p(A) \to \eta X$	18	$\bar{p}^\uparrow p \to \eta X$	25	$K^- p^\uparrow \to \pi^0 X$
5	$p^\uparrow p(A) \to K^- X$	12	$d^\uparrow p(A) \to \pi^+ X$	19	$\bar{p} d^\uparrow \to \pi^0 X$	26	$\pi^- p^\uparrow \to \eta X$
6	$p^\uparrow p \to K^0_S X$	13	$d^\uparrow p(A) \to \pi^- X$	20	$\pi^+ p^\uparrow \to \pi^+ X$	27	$\bar{p} p^\uparrow \to \pi^0 X$
7	$p^\uparrow p(A) \to nX$	14	$p^\uparrow p \to \Lambda X$	21	$\pi^- p^\uparrow \to \pi^- X$	28	-

Single-spin asymmetry A_N

A list of other possible 28 reactions is shown in Table 2 and includes various particles and resonances, for which A_N have not been measured yet. Final decay mode of the detected particle *h* is indicated only in the Table 2.

The initial state can be any with a polarized beam: p↑p, p↑d, d↑p, d↑d.

Table 2. Inclusive reactions to be studied at the SPD for which A_N has not yet been measured. The reaction is $p^{\uparrow}p \to h + X$. Final decay mode of the detected particle h is indicated only.

№	Decay mode	№	Decay mode	№	Decay mode	№	Decay mode
1	$K_L^0 \to \pi^+\pi^-\pi^0$	8	$\omega(782) \to \pi^+\pi^-\pi^0$	15	$\bar{\Lambda} \to \bar{p}\pi^+$	22	$\Delta^{++} \to p\pi^+$
2	$\eta' \to \pi + \pi - \eta$	9	$\omega(782) \to \gamma\pi^0$	16	$\Xi^- \to \Lambda\pi^-$	23	$\Delta^+ \to p\pi^0$
3	$a_0(980) \to \eta\pi^0$	10	$\phi \to K^+K^-$	17	$\Xi^0 \to \Lambda\pi^0$	24	$\Delta^0 \to p\pi^-$
4	$K^{0*}(892) \to K^+\pi^-$	11	$\rho^0(770) \to \pi^+\pi^-$	18	$\bar{\Xi}^+ \to \bar{\Lambda}\pi^+$	25	$\Delta^- \to n\pi^-$
5	$K^{0*}(892) \to K^-\pi^+$	12	$\rho^+(770) \to \pi^+\pi^0$	19	$\bar{\Xi}^0 \to \bar{\Lambda}\pi^0$	26	$\bar{\Delta}^{--} \to \bar{p}\pi^-$
6	$K^{+*}(892) \to K^+\pi^0$	13	$\rho^-(770) \to \pi^-\pi^0$	20	$\Sigma^0 \to \Lambda\gamma$	27	$\bar{\Delta}^- \to \bar{p}\pi^0$
7	$K^{-*}(892) \to K^-\pi^0$	14	$\rho^0(770) \to \mu^+\mu^-$	21	$\bar{\Sigma}^0 \to \bar{\Lambda}\gamma$	28	$\bar{\Delta}^0 \to \bar{p}\pi^+$

Hyperon polarization P_N

Inclusive reactions for which hyperon polarization (P_N) has been measured are shown in Table 3. The first 14 reactions can potentially be studied also in the NICA SPD experiment.

The initial state can be any: p↑p, p↑d, d↑p, d↑d, C+C and Ca+Ca.

Global polarization with respect to the reaction plane of two colliding nuclei can be measured also and compared with P_N.

Table 3. Inclusive reactions for which the polarization (P_N) of hyperons was measured.

№	Reaction	№	Reaction	№	Reaction	№	Reaction
1	$pp(A) \to \Lambda^{\uparrow} X$	9	$pp(A) \to \bar{\Xi}^{+\uparrow} X$	17	$\Sigma^- A \to \Lambda^{\uparrow} X$	25	$\pi^- p \to \Lambda^{\uparrow} X$
2	$pp(A) \to \Xi^{-\uparrow} X$	10	$pp(A) \to \bar{\Xi}^{0\uparrow} X$	18	$\Sigma^- A \to \bar{\Lambda}^{\uparrow} X$	26	$\pi^- p \to \bar{\Lambda}^{\uparrow} X$
3	$pp(A) \to \Xi^{0\uparrow} X$	11	$pp(A) \to \bar{\Sigma}^{-\uparrow} X$	19	$K^- p \to \Lambda^{\uparrow} X$	27	$\pi^+ p \to \Lambda^{\uparrow} X$
4	$pp(A) \to \Sigma^{+\uparrow} X$	12	$A_1 A_2 \to \Lambda^{\uparrow} X$	20	$K^- p \to \bar{\Lambda}^{\uparrow} X$	28	$K^- A \to \Xi^{-\uparrow} X$
5	$pp(A) \to \Sigma^{0\uparrow} X$	13	$A_1 A_2 \to \Lambda^{\uparrow(G)} X$	21	$K^+ p \to \Lambda^{\uparrow} X$	29	$\bar{p} A \to \bar{\Lambda}^{\uparrow} X$
6	$pp(A) \to \Sigma^{-\uparrow} X$	14	$A_1 A_2 \to \bar{\Lambda}^{\uparrow(G)} X$	22	$K^+ p \to \bar{\Lambda}^{\uparrow} X$	30	$e^+ e^- \to \Lambda^{\uparrow} X$
7	$pp(A) \to \Omega^{-\uparrow} X$	15	$\Sigma^- A \to \Sigma^{+\uparrow} X$	23	$\pi^- A \to \Xi^{-\uparrow} X$	31	$\nu_\mu A \to \Lambda^{\uparrow} X$
8	$pp(A) \to \bar{\Lambda}^{\uparrow} X$	16	$\Sigma^- A \to \Xi^{-\uparrow} X$	24	$\pi^- A \to \bar{\Xi}^{+\uparrow} X$	32	$e^+ A \to \bar{\Lambda}^{\uparrow} X$

Physical motivation

It is important to note that for hyperons it is possible to simultaneously measure both the transverse polarization P_N and the single-spin asymmetry A_N. Comparing A_N and P_N for a specific reaction with the predictions of various models will bring us closer to revealing the mechanism of the origin of polarization phenomena at high energies and will shed light on the physics of strong interactions in the confinement region.

Data on dozens of reactions have been accumulated, but the accuracy of measurements and the limited kinematic region in most experiments do not yet allow unambiguous conclusions to be drawn about the origin of polarization phenomena and even about their dependence on various variables (p_T, x_F, $\sqrt{s}$, A_1, A_2, N_{ch}, flavor, isospin, spin).

The purpose of this proposal is to significantly expand the amount of polarization data available for analysis and to improve their accuracy. This will help advance the creation of adequate models of polarization phenomena and their discrimination when compared with the entire dataset. Global analysis of the entire dataset is suggested.

Model of chromomagnetic polarization of quarks (CPQ)

It is assumed in the CPQ model, that there is a circular transverse chromomagnetic field $\mathbf{B}^a$ in the interaction region. It is created by relativistic spectator quarks, moving forward and backward in c.m. $\boldsymbol{\mu}^a_Q = s g^a g_s / 2M_Q$ – the chromomagnetic dipole moment of the constituent quark Q interacts with the inhomogeneous chromomagnetic field (Stern-Gerlach force arises). Stern-Gerlach force acts on a test quark (which will be a part of a hadron) and gives it a Pt kick to the left or right, for quark spin UP or DN. **The quark spin precession in the chromomagnetic field $\mathbf{B}^a$ changes the Stern-Gerlach force components and this leads to an oscillation of P_N or A_N as a function of its arguments (x_F, p_T) in the case of strong enough field. Attraction between test and spectator quarks can lead to "resonance" type energy dependence for $A_N(\sqrt{s})$ and $P_N(\sqrt{s})$. In the CPQ model the interaction region can be considered as a microscopic Stern-Gerlach apparatus:**

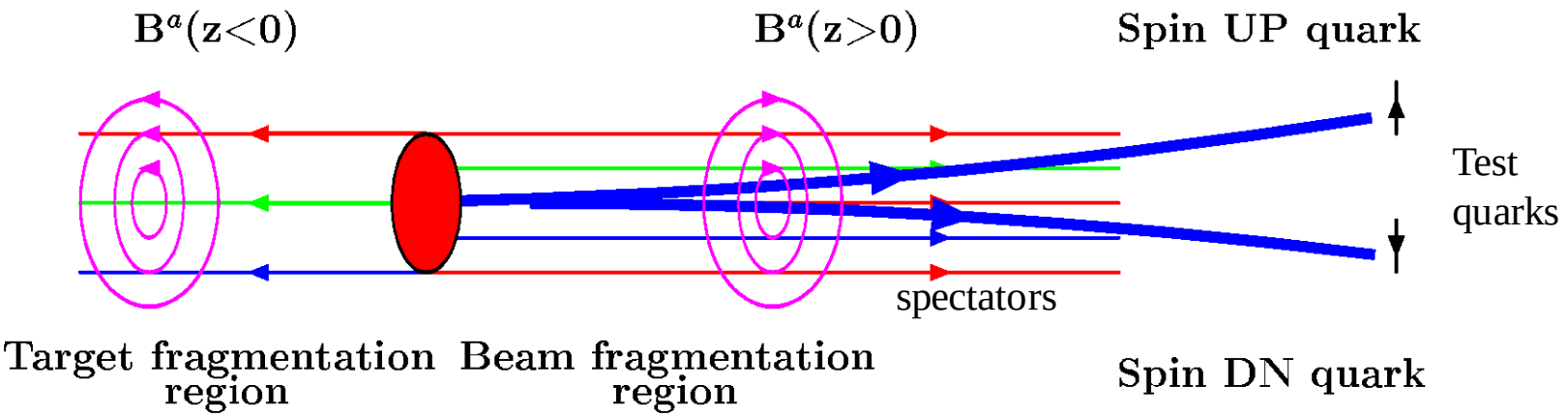

Equations for A_N, P_N and $(\rho_{00}-1/3)$

$$P_N \approx C(\sqrt{s})\, F(p_T, A)[G(\varphi_A) - \sigma G(\varphi_B)], \quad (3)$$

$$G(\varphi_A) = [1 - \cos\varphi_A]/\varphi_A + \varepsilon\varphi_A, \quad (4)$$

spin precession and S-G force,

where $\varepsilon = -0.00497 \pm 0.00009$ - global, σ – local parameter.

$$C(\sqrt{s}) = v_0/[(1 - E_R/\sqrt{s})^2 + \delta_R^2]^{1/2}, \quad (5)$$

spin precession vs E_Q

$$F(p_T, A) = \{1 - \exp[-(p_T/p^0_T)^{2.5}]\}(1 - \alpha_A \ln A), \quad (6)$$

color form factor

$$v_0 = -D_r\, g^a_Q\, P_Q /2(g^a_Q - 2), \quad (7)$$

sign and magnitude of A_N and P_N

$$\varphi_A = \omega^0_A y_A, \quad \varphi_B = \omega^0_B y_B, \quad (8)$$

integral "precession angles"

$$y_A = x_A - (E_0/\sqrt{s} + f_0)[1 + \cos\theta_{cm}] + a_0[1 - \cos\theta_{cm}], \quad (9)$$

$$y_B = x_B - (E_0/\sqrt{s} + f_0)[1 - \cos\theta_{cm}] + a_0[1 + \cos\theta_{cm}], \quad (10)$$

$$x_A = (x_R + x_F)/2, \quad x_B = (x_R - x_F)/2. \quad (11)$$

scaling variables

$$\omega^0_{A(B)} = g_s \alpha_s \nu_{A(B)}\, m_r (g^a_Q - 2)/M_Q, \quad m_r = 0.2942 \pm 0.0072\ \text{GeV}. \quad (12)$$

$\nu_{A(B)}$ - effective contributions of the spectator quarks to the field B^a.

Oscillation of A_N and P_N in a strong color field

$$P_N \approx C(\sqrt{s})\, F(p_T, A)[G(\varphi_A) - \sigma G(\varphi_B)], \quad (3)$$

$$G(\varphi_A) = [1 - \cos\varphi_A]/\varphi_A + \varepsilon\varphi_A, \quad (4)$$

is a result of the spin precession and S-G force

were φ_A, φ_B – are the integral "spin precession angles" in the fragmentation regions of the projectile A and the target B, respectively. $\varepsilon = -0.00497 \pm 0.00009$.
Analysis shows that effective length S of the field B^a is: $S_0 x_A$ or $S_0 x_B$ for fragmentation regions of colliding particles A and B, where S_0 is about 1 fm.

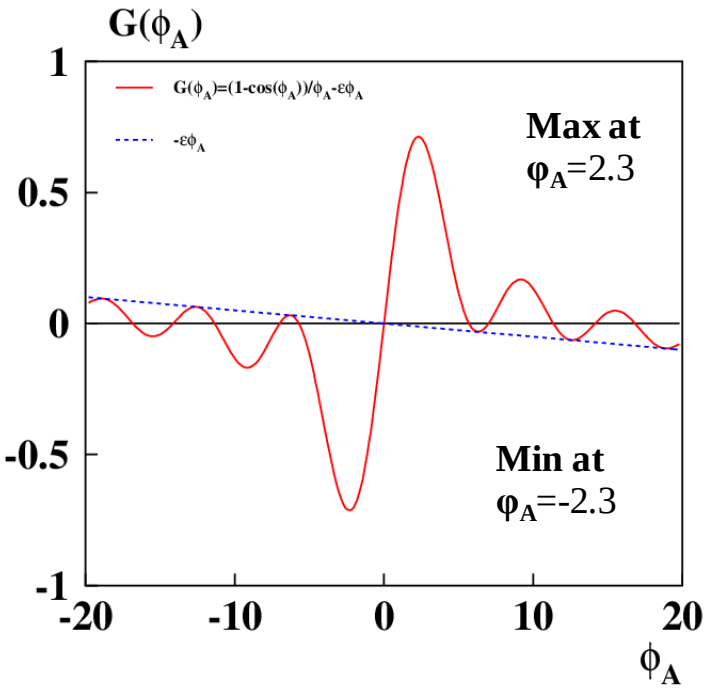

$$\varphi_A = \omega^0_A y_A, \quad \varphi_B = \omega^0_B y_B; \quad (8)$$

$$\omega^0_{A(B)} = g_s \alpha_s \nu_{A(B)}\, m_r (g^a_Q - 2)/M_Q, \quad (12)$$

$$m_r = 0.2942 \pm 0.0072\ \text{GeV}; \quad \alpha_s = g_s^2/4\pi;$$

$$y_A = x_A - (E_0/\sqrt{s} + f_0)[1 + \cos\theta_{cm}] + a_0[1 - \cos\theta_{cm}] \quad (9)$$

$$y_B = x_B - (E_0/\sqrt{s} + f_0)[1 - \cos\theta_{cm}] + a_0[1 + \cos\theta_{cm}] \quad (10)$$

$x_A = (x_R + x_F)/2$, $x_B = (x_R - x_F)/2$ - scaling variables. (11)

$\nu_{A(B)}$ - effective contributions of the spectator quarks to the field B^a.

"Resonance" dependence of $A_N(\sqrt{s})$ and $P_N(\sqrt{s})$

$$P_N \approx C(\sqrt{s})\, F(p_T, A)[G(\varphi_A) - \sigma G(\varphi_B)], \quad (3)$$

$$C(\sqrt{s}) = v_0/[(1 - E_R/\sqrt{s})^2 + \delta_R^2]^{1/2}, \quad (5)$$

Possible explanations of the "resonance" type eq. (5):

1) Dependence of quark spin precession frequency on its energy E_Q. Spin precession frequency ~ $(g^a_Q - 2 + 2M_Q/E_Q)$ is 0 at some E_Q and A_N or P_N reach their maximum magnitudes at $\sqrt{s} = E_R$.

2) Attraction of test and spectator quarks. For attraction case $E_R > 0$, and for repulsion case $E_R < 0$.

The sign of E_R is given by expression $-g_S \nu_A P_Q$, where g_S is the test quark color charge, P_Q – polarization of a test quark Q, and ν_A is the number of spectator quarks and antiquarks with weights according to quark counting rules or quark diagrams in a fragmentation region of a projectile A.

An example of reactions with $E_R > 0$ are $p + p \rightarrow \tilde{\Lambda} + X$ and $p + p \rightarrow \tilde{\Xi}^+ + X$, and reaction with $E_R < 0$ is $p + p \rightarrow \Xi^- + X$. The global data fit confirms the E_R sign rule for most of 85 reactions (96.5%).

Quark counting rules for $p\uparrow + p \rightarrow \pi^+ + X$

$\nu_A = 3\lambda - 3\tau\lambda = -0.398$ (3)

$\nu_B = \nu_A$, where global parameters for 85 (3608 points) reactions are:

$\lambda = -0.1363 \pm 0.0003$, (4)

$\tau = 0.0267 \pm 0.0005$. (5)

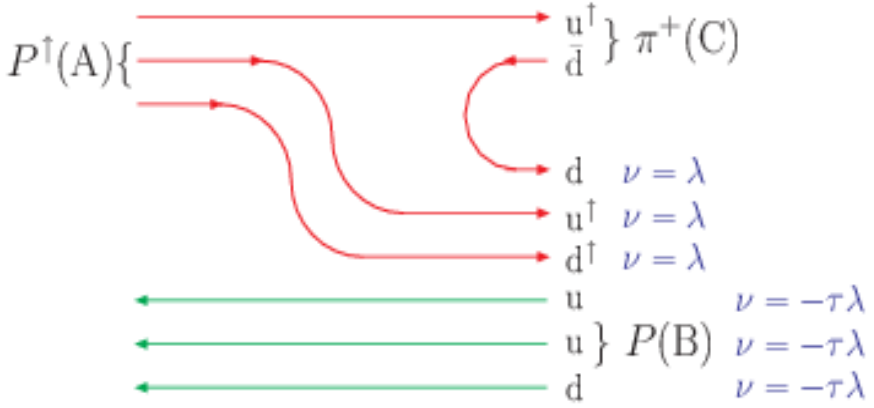

SPECTATORS

For comparison is shown a quark flow in reaction $p\uparrow + p \rightarrow p + X$.

The effective number of quarks is:

$\nu_A = 2 + 2\lambda - 3\tau\lambda = 1.738$, (6)

$\nu_B = \nu_A$.

So, in case of reaction $p\uparrow + p \rightarrow p + X$ ν_A is approximately 4 times higher, than in case of $p + p \rightarrow \pi^+ + X$. As a result, $A_N(x_F)$ should oscillates with approximately 4 times higher frequency for $p\uparrow + p \rightarrow p + X$ reaction. The sign $(-g_S \nu_A P_Q)$ of A_N for proton must be opposite (negative) at small x_F.

and $p\uparrow + p \rightarrow p + X$

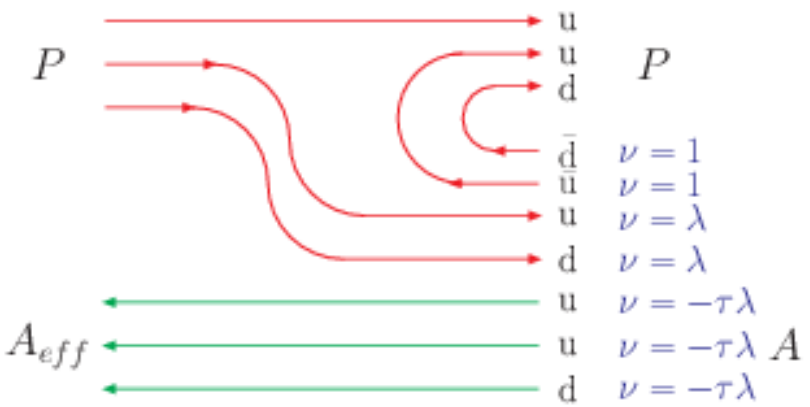

SPECTATORS

The role of color factor λ

When taking into account the interaction of a test quark with the field created by a moving spectator quark, it is necessary to take into account the color factor for the corresponding pair of quarks (spectator and test quarks). An analysis of the data have shown that the quark-antiquark pair interacts predominantly in the color-singlet state with the color factor $\mathbf{C_F = 4/3}$, and the quark-quark or antiquark-antiquark pair interacts in the color-triplet state with $\mathbf{C_F = 2/3}$. For a hydrogen-like potential, the wave function of two quarks or a quark and an antiquark at zero coordinate is proportional to $\mathbf{|\Psi(0)| \sim (C_F \alpha_S)^{3/2}}$ [7], which leads to the ratio of contributions from qq and $q\tilde{q}$ interactions to ν_A of the order

$$\mathbf{\lambda \approx -|\Psi qq(0)|^2/|\Psi q\tilde{q}(0)|^2 = -1/8.} \qquad (1)$$

The minus sign in (1) takes into account the opposite sign of the field created by a moving spectator quark and a moving spectator antiquark. Experimentally, the value of the global parameter **λ**, obtained as a result of the global fit of the polarization data, turned out to be $\mathbf{\lambda = -0.1363 \pm 0.0003}$. A value, more close to the experimental one is given by the formula $\lambda = 1 - \exp(1/8) \approx -0.1331$, which can be considered as a generalization of formula (1).

[7] Baranov S.P. On the production of doubly flavored baryons in p p, e p and gamma gamma collisions // Phys. Rev. — 1996. — V. D54 — P. 3228–3236.

$A_N(x_F)$ for $p\uparrow + p \rightarrow \pi^+ + X$

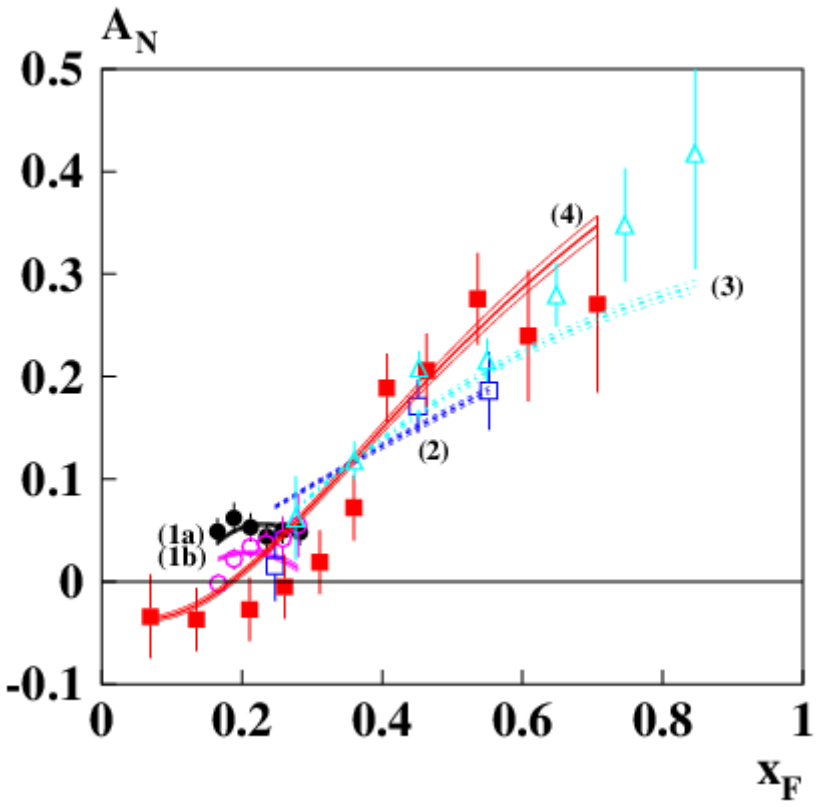

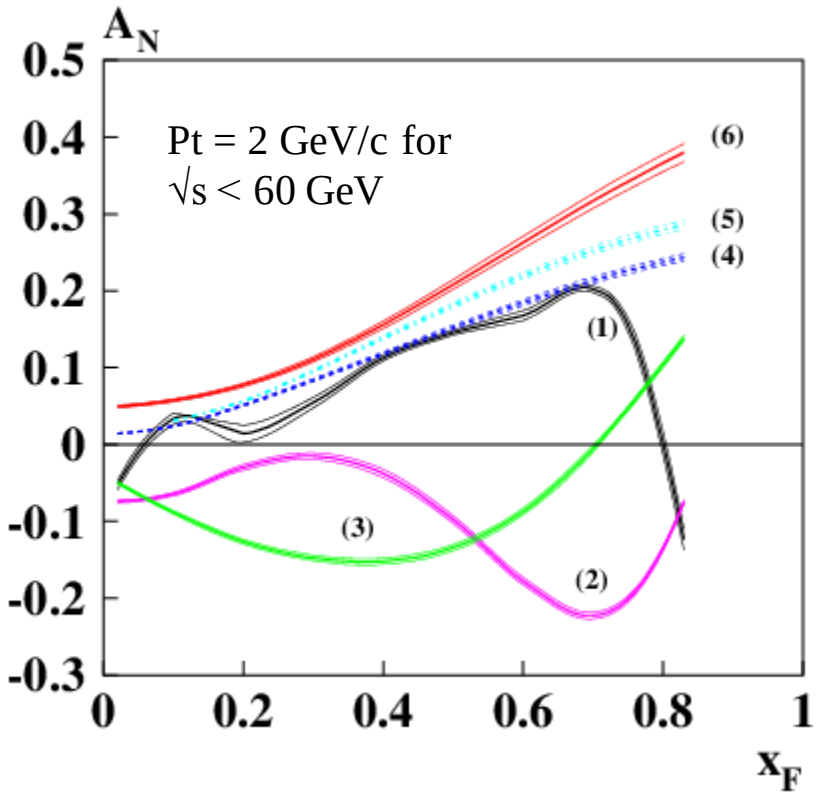

Different energy data and the CPQ model calculations from V.V. Abramov, J. Phys. Conf. Ser. 678 (2016) 012039. Left panel: $A_N(x_F)$ data for $\sqrt{s}$ = 200 (1), 64.2 (2), 19.4 (3) and 8.77 (4) GeV. Right panel: $A_N(x_F)$ calculations are performed for $\sqrt{s}$ = 500 (1), 200 (2), 130 (3), 64.2 (4), 19.4 (5) and 8.77 (6) GeV.

Near linear $A_N(x_F)$ dependence for $\sqrt{s} < 70$ GeV is due to a small $\mathbf{\nu_A = -0.398}$.

The sign of $A_N > 0$ since $\mathbf{A_N \sim -g_s \nu_A P_u > 0}$, where P_u is u-quark polarization.

$A_N(x_F)$ for $p\uparrow + p \rightarrow \pi^- + X$

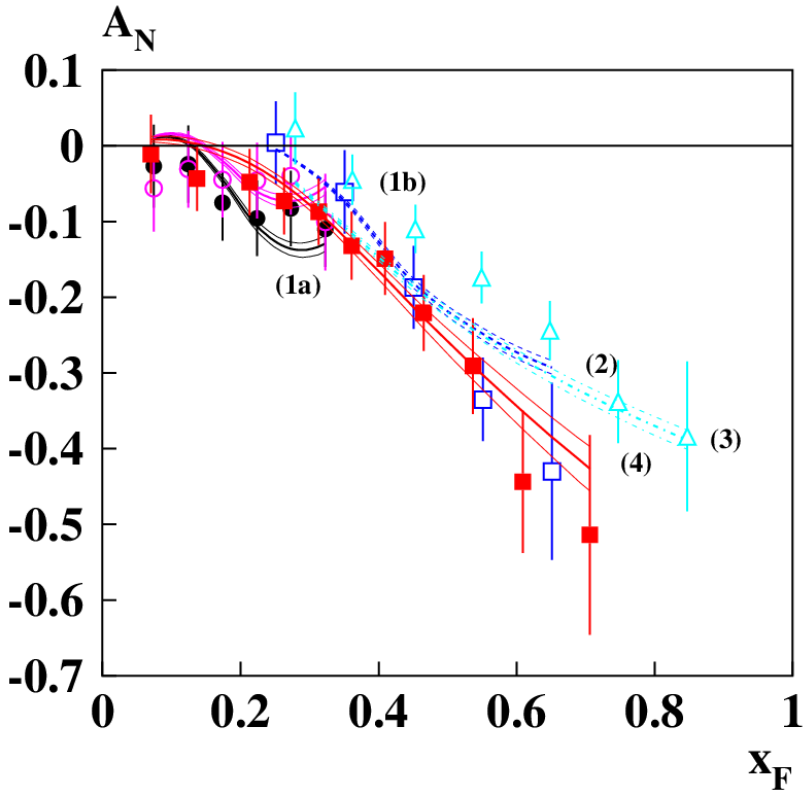

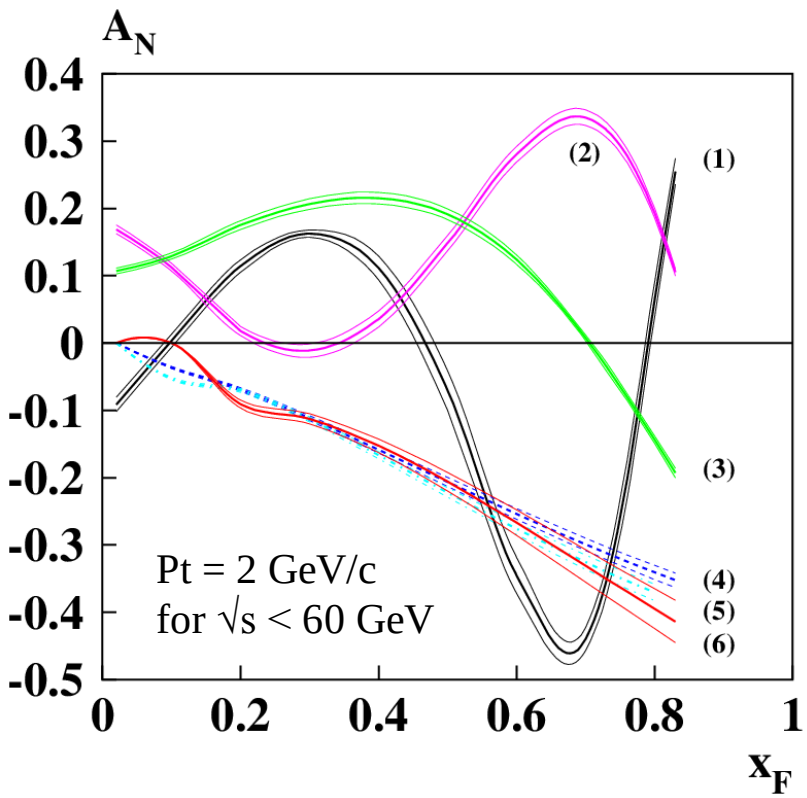

Different energy data and the CPQ model calculations from V.V. Abramov, J. Phys. Conf. Ser. 678 (2016) 012039. Left panel: $A_N(x_F)$ data for $\sqrt{s}$ = 200 (1), 64.2 (2), 19.4 (3) and 8.77 (4) GeV. Right panel: $A_N(x_F)$ calculations are performed for $\sqrt{s}$ = 500 (1), 200 (2), 130 (3), 64.2 (4), 19.4 (5) and 8.77 (6) GeV.

Near linear $A_N(x_F)$ dependence for $\sqrt{s} < 70$ GeV is due to a small $\mathbf{\nu_A = -0.398}$.

The sign of $A_N < 0$ since $\mathbf{A_N \sim -g_s \nu_A P_d < 0}$, where P_d is d-quark polarization.

$A_N(x_F)$ for $p\uparrow + p \rightarrow p + X$

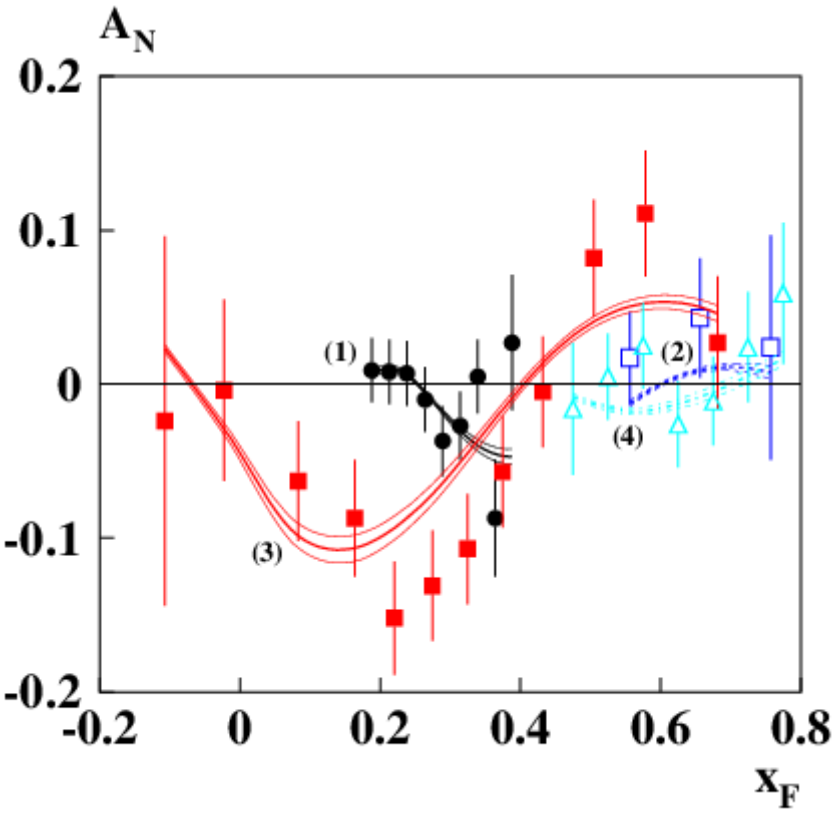

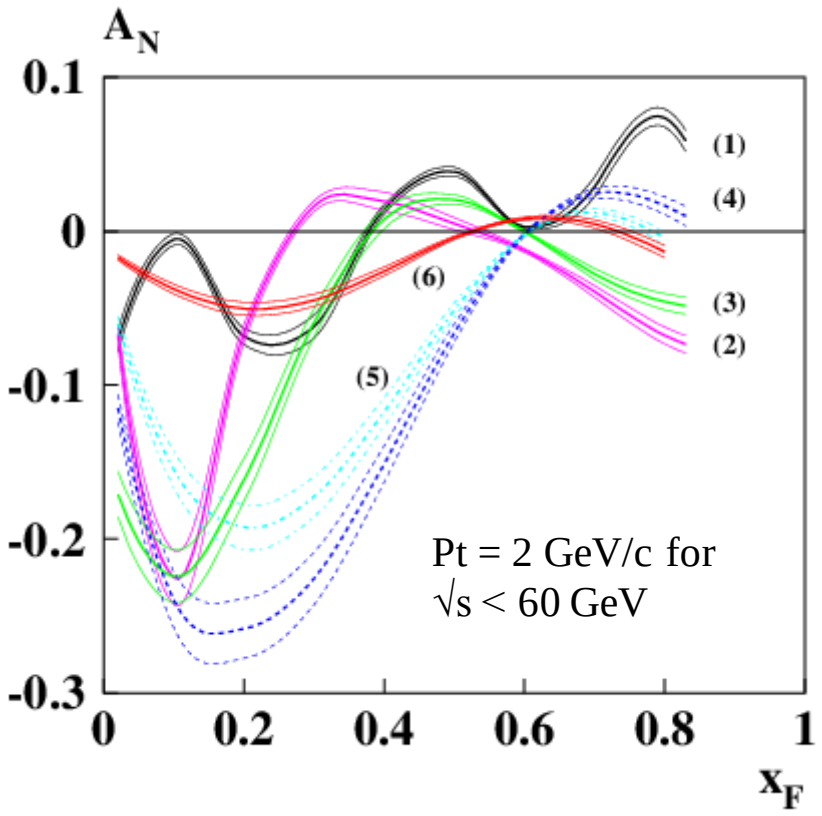

Different energy data and the CPQ model calculations from V.V. Abramov, J. Phys. Conf. Ser. 678 (2016) 012039. Left panel: $A_N(x_F)$ data for $\sqrt{s}$ = 200 (1), 64.2 (2), 8.77 (3) and 6.51 (4) GeV. Right panel: $A_N(x_F)$ calculations are performed for $\sqrt{s}$ = 500 (1), 200 (2), 130 (3), 64.2 (4), 19.4 (5) and 8.77 (6) GeV. The sign of $A_N < 0$ since $\mathbf{A_N \sim -g_s \nu_A P_u < 0}$. Oscillating $A_N(x_F)$ dependence is due to a large $\nu_A = +1.738$.

θ_{cm} angle threshold effect for $A_N(y_A)$ in $p\uparrow + p \rightarrow \pi^- + X$

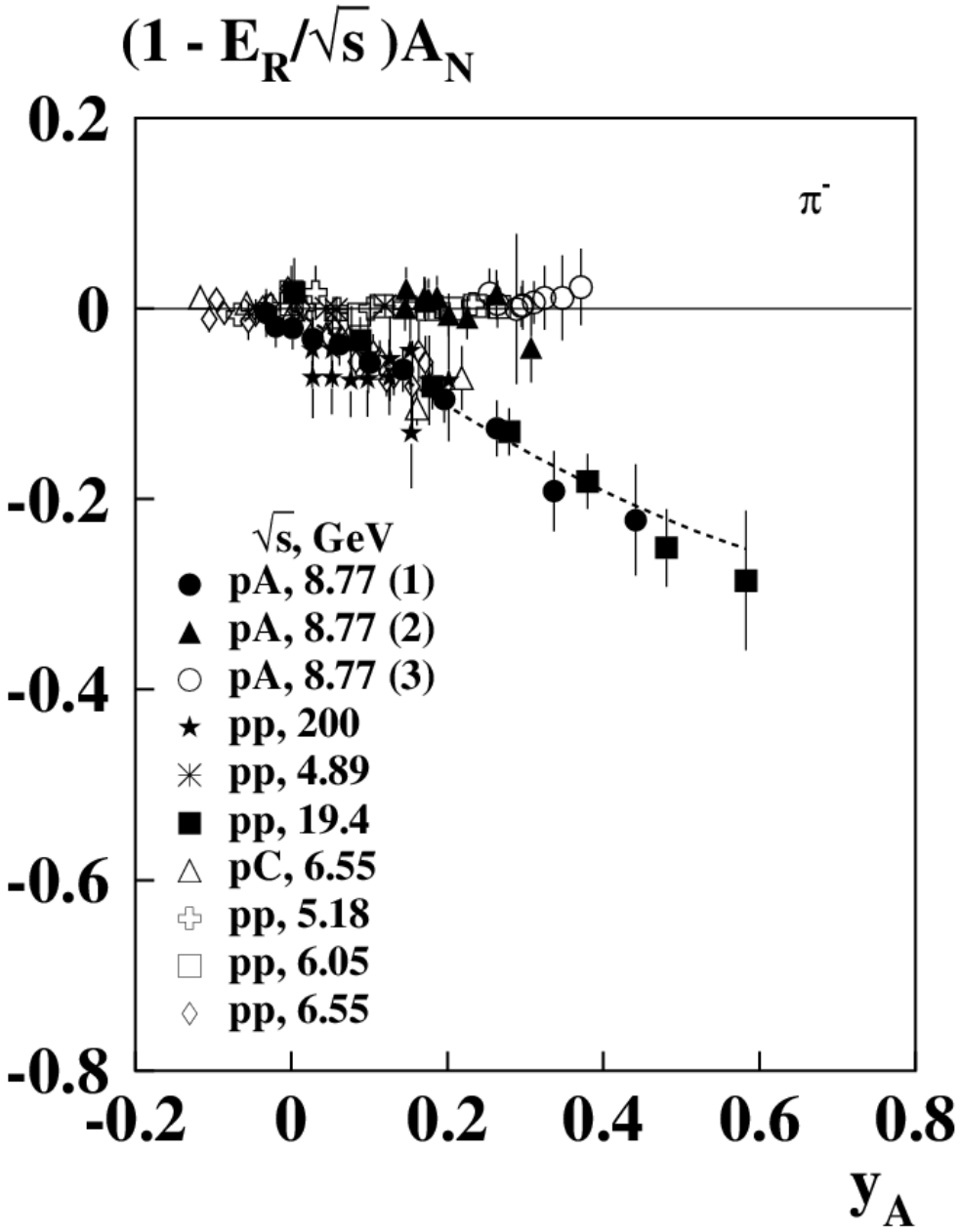

A very unexpected and interesting feature of the reaction $p\uparrow + p \rightarrow \pi^- + X$ turned out to be the threshold dependence of the quantity $(1 - E_R/\sqrt{s})A_N$ on y_A, where $\mathbf{E_R = 4.98 \pm 0.29\ GeV}$. It turned out that this quantity is described by the universal scaling function of y_A, if $\theta_{cm} < 74^o$, and is equal to zero if $\theta_{cm} > 74^o$.

In figure two clearly distinct branches are visible, into which the experimental points are grouped.

Qualitatively, this can be explained by the greater mass of the *d*-quark in comparison with the average mass of the constituent quarks in the proton. The polarized *d*-quark is scattered mainly on the light *u*-quark at an angle less than 90^o. The opposite case should be for reaction $p\uparrow + p \rightarrow \pi^+ + X$, where light a polarized *u*-quark can scatter on angle more or equal 90^o.

The factor $(1 - E_R/\sqrt{s})$ demonstrates the "resonant" energy dependence of A_N $(\sqrt{s})$.

θ_{cm} angle threshold effect for $A_N(y_A)$ in $p\uparrow + p \rightarrow \pi^+ + X$

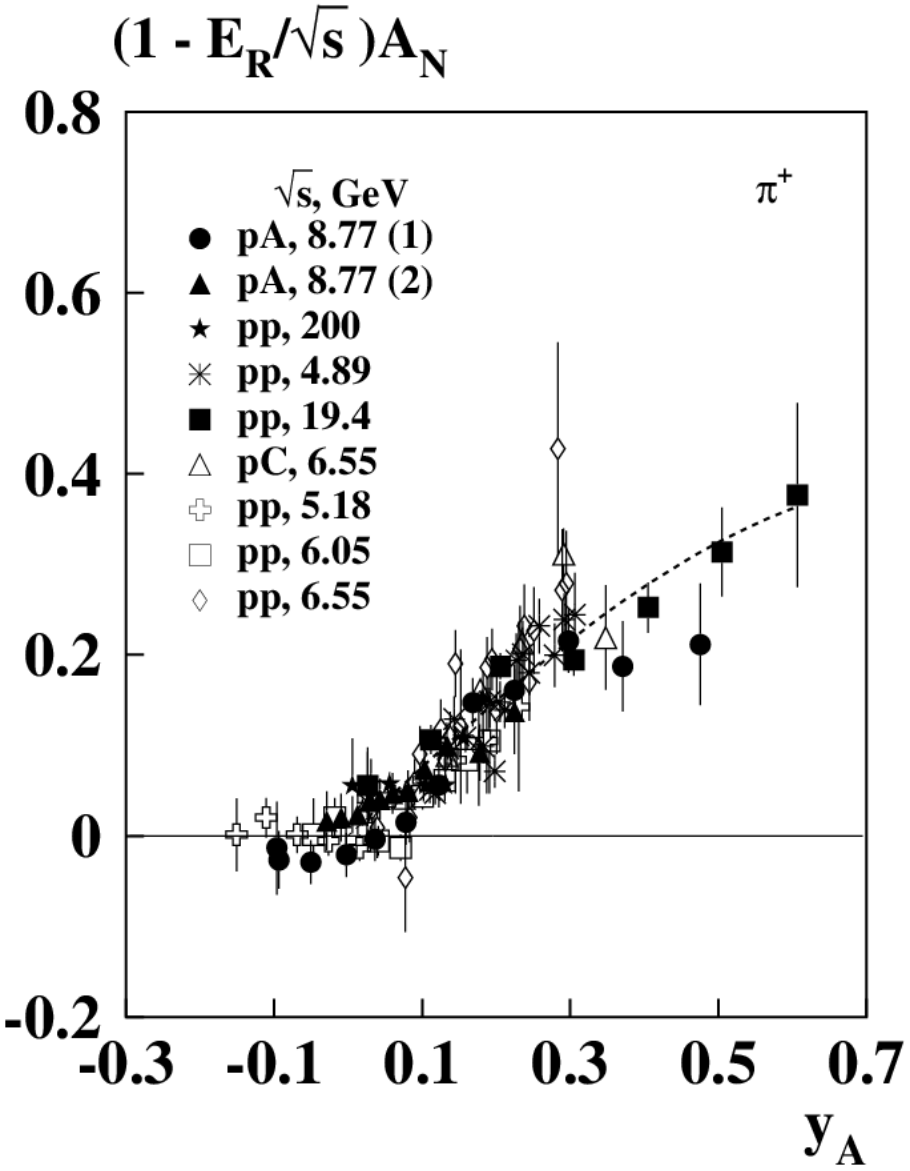

The dependence of the quantity $(1 - E_R/\sqrt{s})\,A_N$ on y_A is shown for the reaction $p\uparrow + p \rightarrow \pi^+ + X$, where $\mathbf{E_R = 1.92 \pm 0.30\ GeV}$. This quantity is described by the universal scaling function of y_A for all angles $\theta_{cm} < 90^o$. Experimental points are grouped into one branch.

A positive E_R value is a manifestation of the "attraction" effect of test quarks and spectator quarks and a "resonance" energy dependence of $A_N(\sqrt{s})$.

According to formula (5), $A_N(\sqrt{s})$ reaches its maximum value at energy $\sqrt{s} \approx E_R$.

In the framework of the CPQ model, scaling in polarization phenomena is due to the occurrence of processes at the quark level, in the limit of high energies and large transverse momentum.

Abramov V.V. -- Phys. Atom. Nucl. V.70, no.12. -- P. 2103--2112.

Quark counting rules for the p + p → Ξ⁻ + X

$\nu_A = (2 + 2\lambda) - 3\tau\lambda = 1.738$ (3)

$\nu_B = \nu_A$, where global parameters for 85 reactions are:

$\lambda = -0.1363 \pm 0.0003$,

$\tau = 0.0267 \pm 0.0005$.

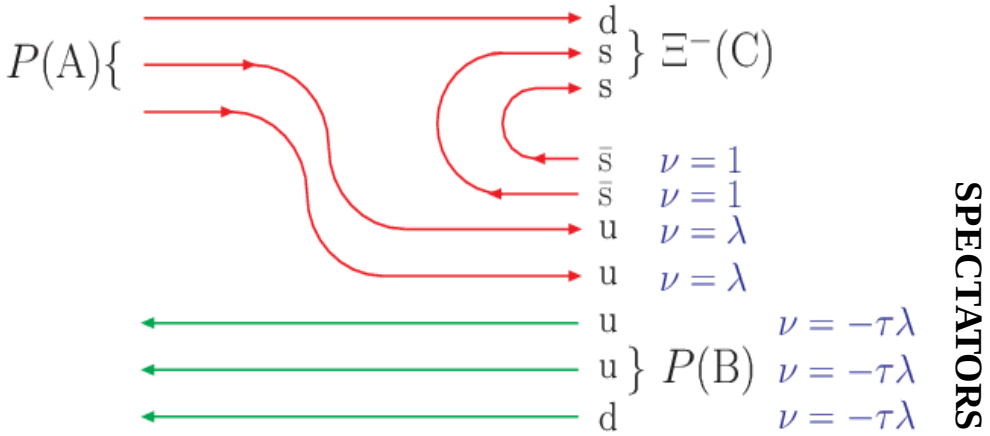

For comparison is shown a quark flow in reaction p + p → Λ + X.

The effective number of quarks is:

$\nu_A = (1 + \lambda) - 3\tau\lambda = 0.8746$ (4)

$\nu_B = \nu_A$.

So, in case of reaction p + p → Ξ⁻ + X ν_A is approximately two times higher, than in case of p + p → Λ + X.

As a result, $P_N(x_F)$ should oscillates with approximately two times higher frequency for p + p → Ξ⁻ + X reaction.

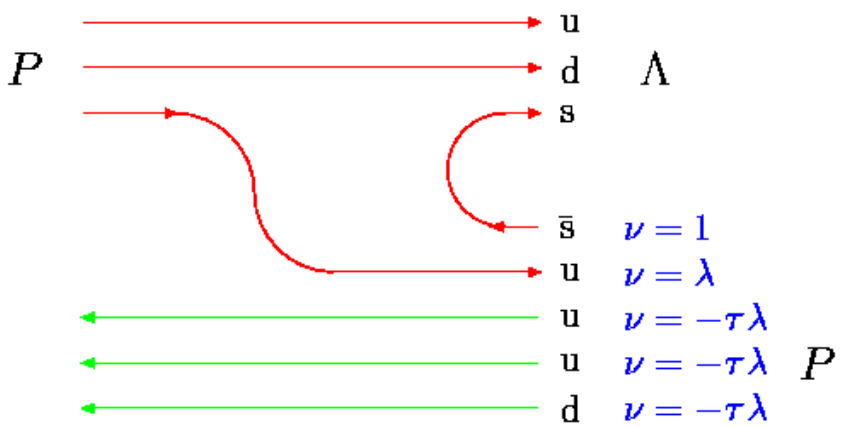

pp → Λ + X production quark diagram.

Color flux tube counting.

“Oscillating” behavour of A_N and P_N

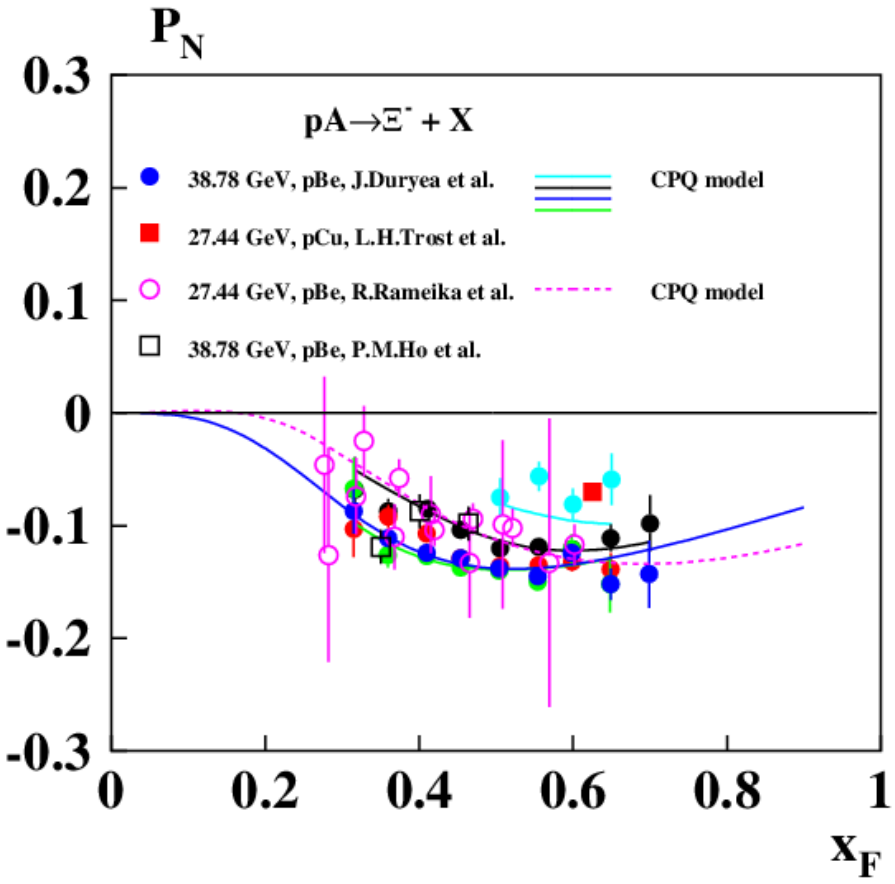

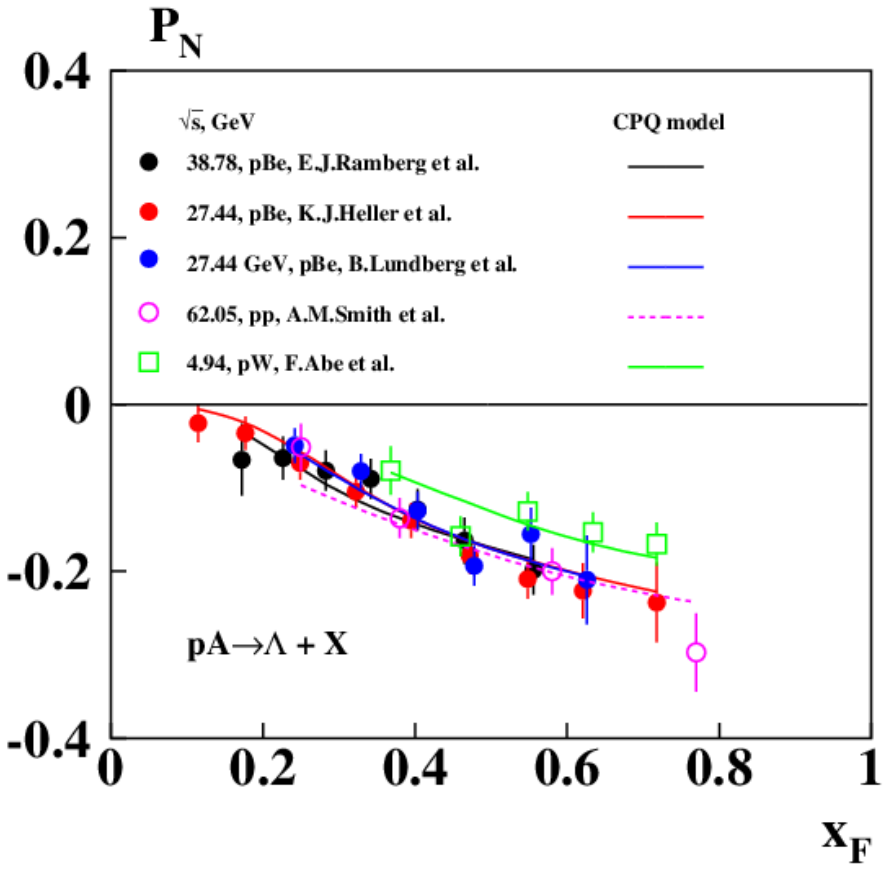

We can see, that $P_N(x_F)$ for the $p + A \rightarrow \Xi^- + X$ reaction is not monotonic (it oscillates) with maximum near $x_F \approx 0.5 - 0.6$, while in case of the $p + A \rightarrow \Lambda + X$ reaction it increases almost linearly up to $x_F \approx 0.75$, due to the smaller value of ν_A. The data is in agreement with the CPQ model predictions, shown by curves.

The sign of $P_N < 0$ since $\mathbf{P_N \sim -g_s \nu_A < 0.}$

The existing data for the p + A → Ξ^0 + X reaction

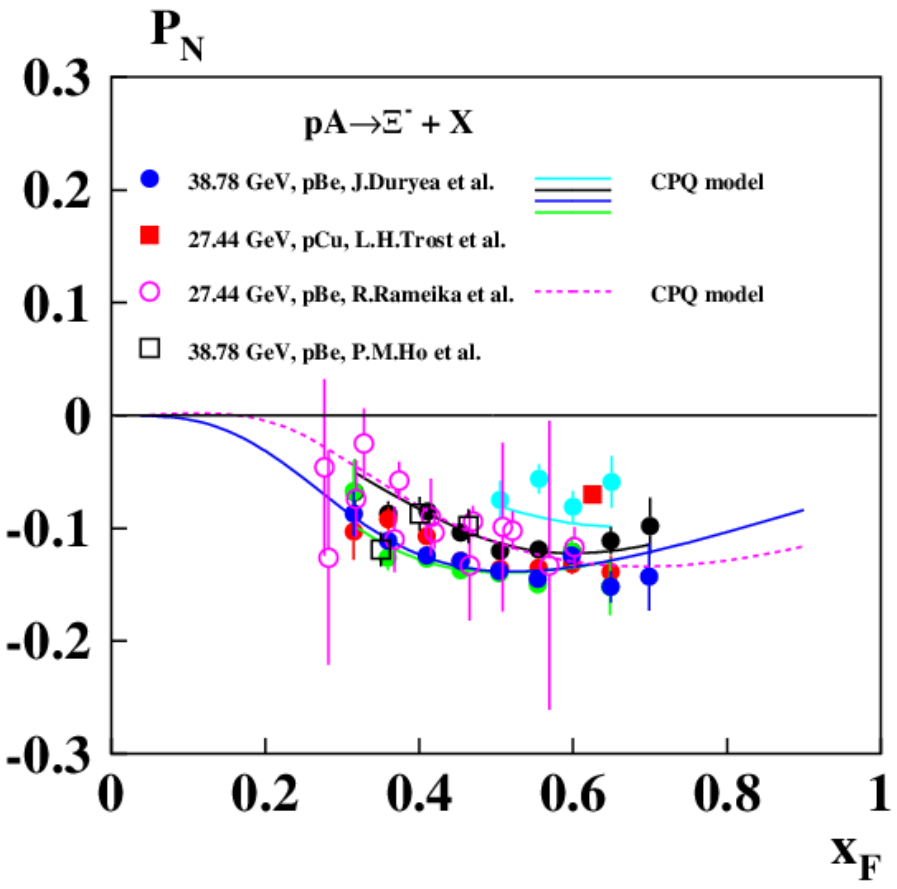

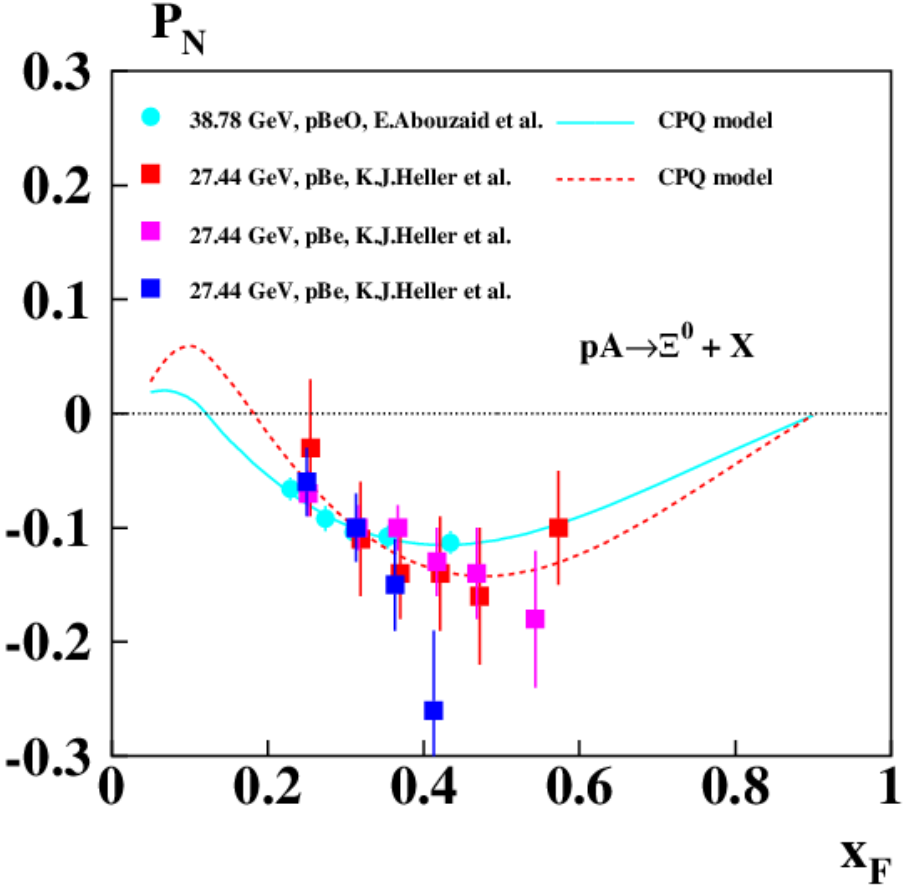

$P_N(x_F)$ for the p + A → Ξ^0 + X reaction looks similar (it oscillates), as in case of the p + A → Ξ^- + X reaction. The magnitude of $P_N(x_F)$ is near its maximum near $x_F \approx 0.4$ - 0.5. This is due to a smaller mass of u-quark (in Ξ^0) in comparison to d-quark (in Ξ^-).

Quark flow diagrams for the cascade antihyperon production

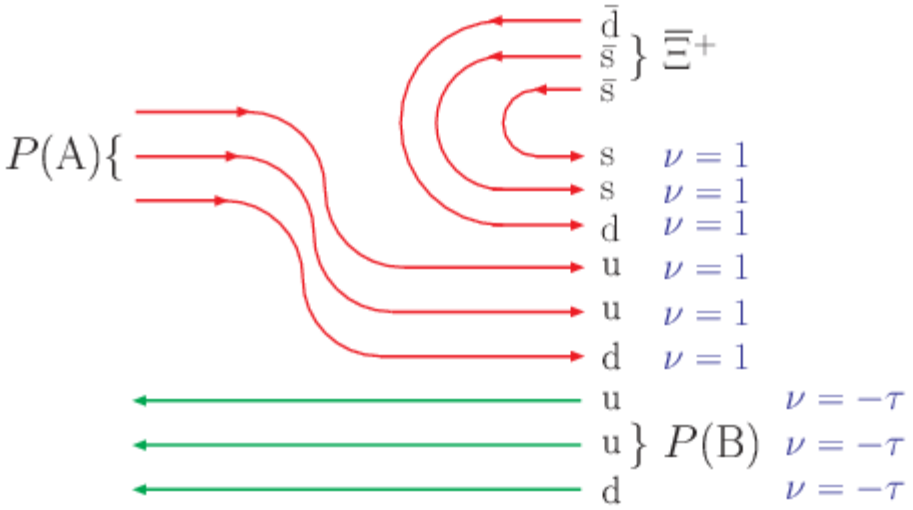

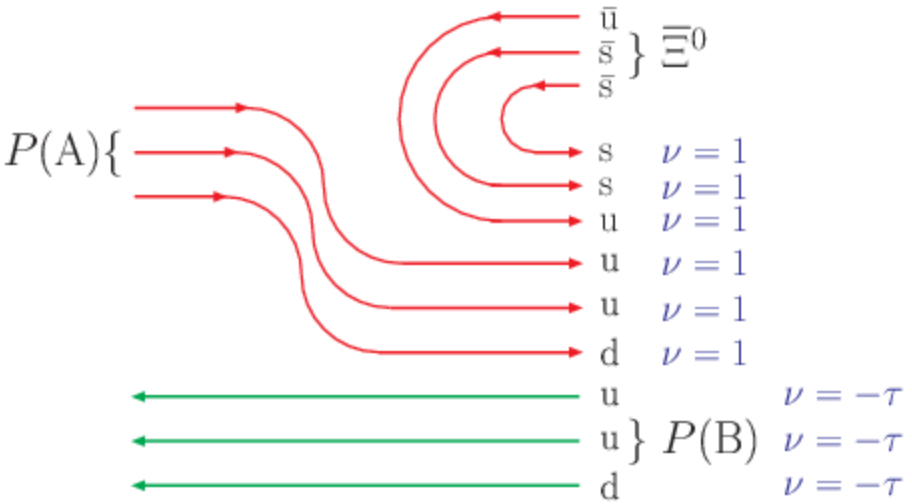

In case of $\bar{\Xi}^+$ and $\bar{\Xi}^0$ production in pA-collisions the quark flow diagrams look similar. But constituent masses of u and d are different.

Six spectator quarks interact with each of active valence test quark of antihyperon and create a very strong chomomagnetic field.

Large values of $\nu_A = \nu_B = 6 - 3\tau$ leads to a very high quark spin precession frequency and the corresponding high oscillation frequency $\boldsymbol{\omega^0_{A(B)}}$ for $P_N(x_F)$, which is proportional to ν_A or ν_B.

The data for cascade antihyperon polarization

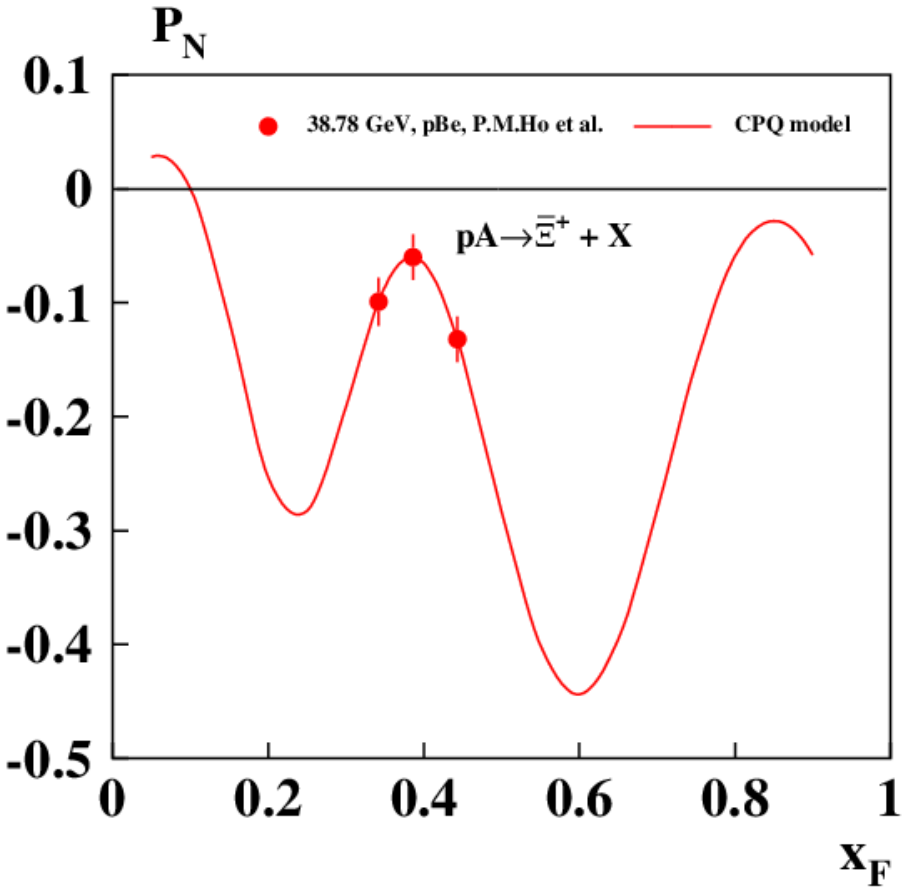

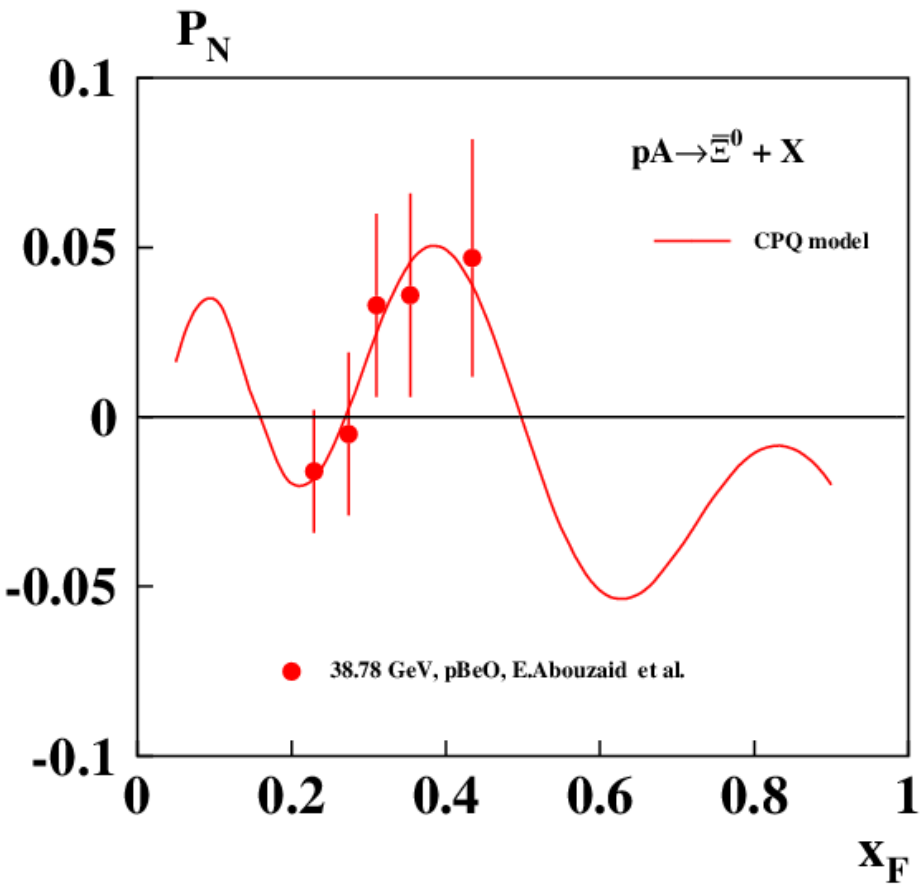

We can see, that $P_N(x_F)$ for the cascade antihyperon production in pA-collisions is not monotonic (it oscillates) with higher frequency, than in case of the corresponding hyperons. The CPQ model agrees with data and predicts several maxima and minima of $P_N(x_F)$. This is the main signature of the CPQ model.

Predictions for the cascade hyperon polarization

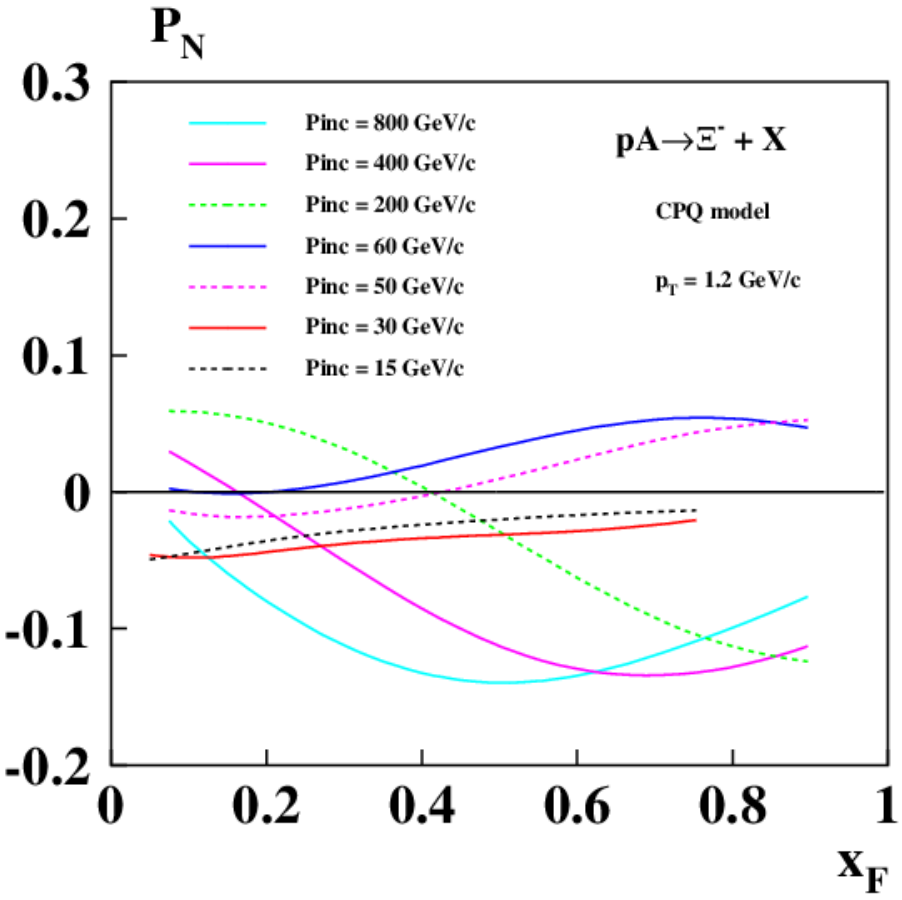

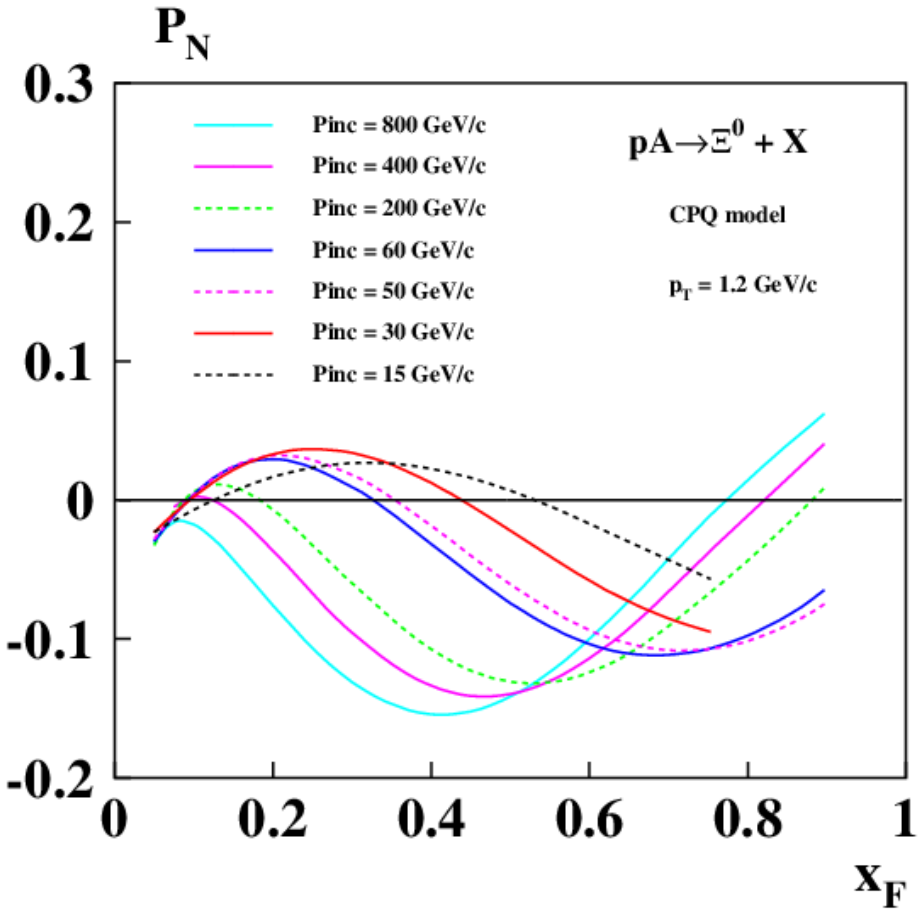

Calculations of $P_N(x_F)$ for the $p + A \rightarrow \Xi^- + X$ and $p + A \rightarrow \Xi^0 + X$ reactions are shown above for p_T = 1.2 GeV/c (near maxima of $|P_N(x_F,p_T)|$). In order to reveal $P_N(x_F)$ oscillation, measurements have to be performed in a wide range of x_F. When beam momentum increases, the $P_N(x_F)$ can reach significant negative value near -0.14. Positive $P_N(x_F)$ are expected at some values of x_F.

Predictions for the cascade antihyperon polarization

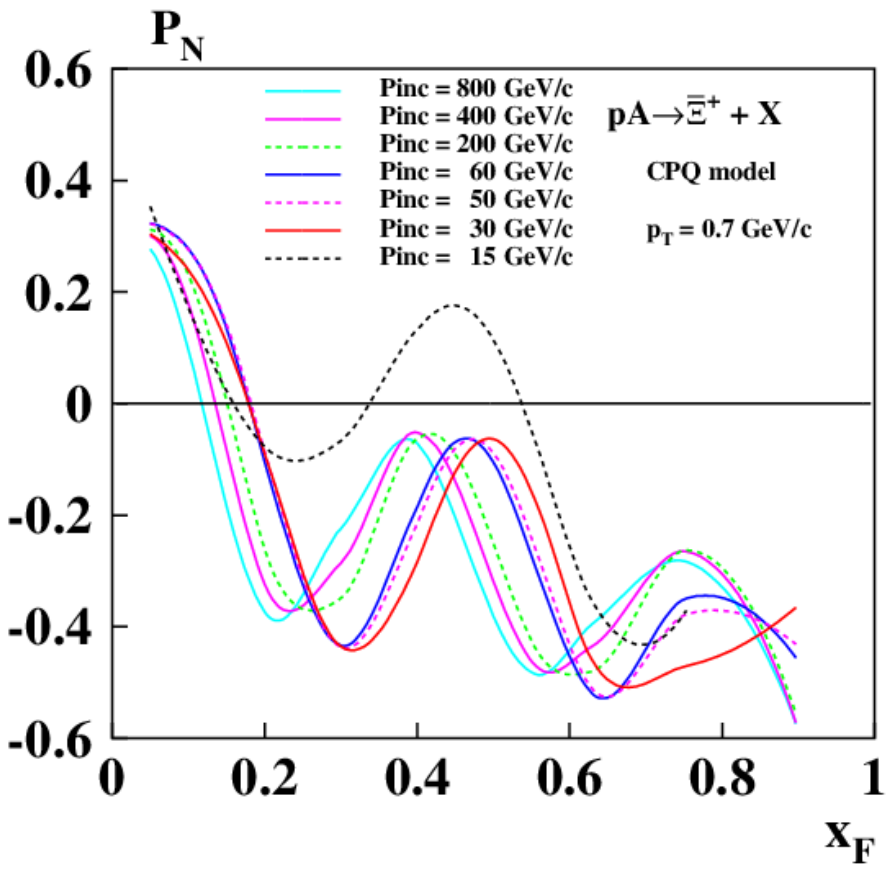

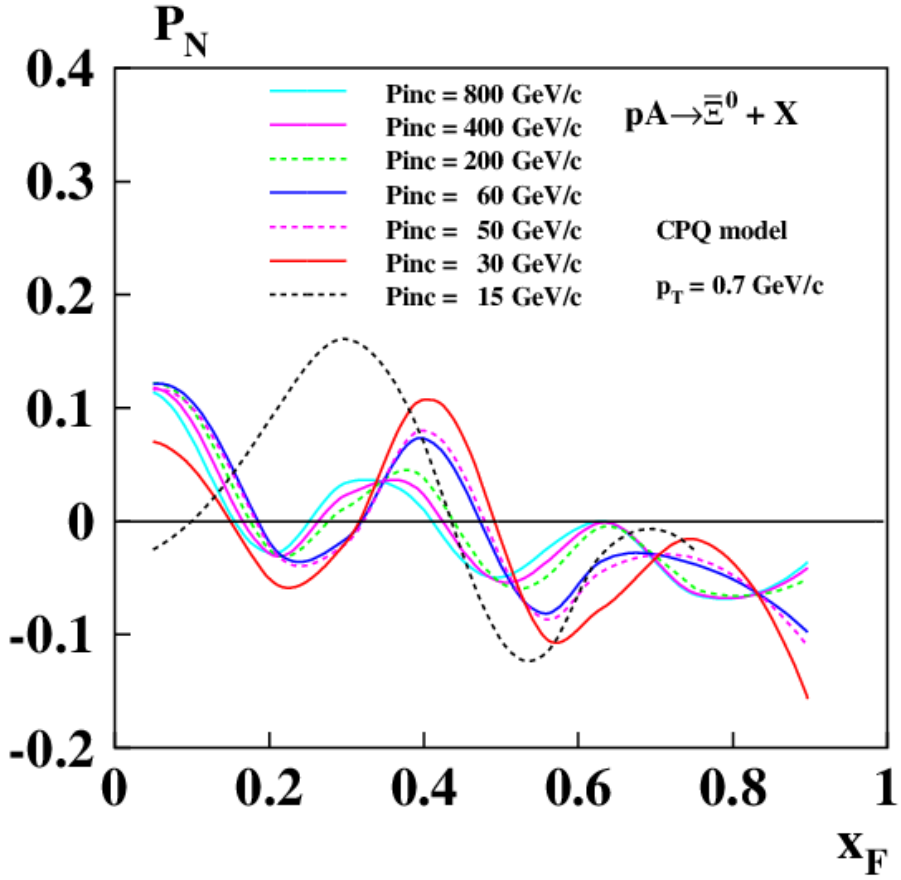

Calculations of $P_N(x_F)$ for the $p + A \to \bar{\Xi}^+ + X$ and $p + A \to \bar{\Xi}^0 + X$ reactions are shown above for $p_T = 0.7$ GeV/c (near maxima of $|P_N(x_F,p_T)|$). In order to reveal the $P_N(x_F)$ oscillation, measurements have to be performed in a wide range of x_F. When beam momentum increases, the position of peaks for $P_N(x_F)$ moves to a smaller x_F. Oscillation of $P_N(x_F)$ is a major CPQ model prediction, related to a quark spin precession in a strong chromomagnetic field in the interaction region.

Polarization predictions for p + A → $\tilde{\Lambda}$ + X

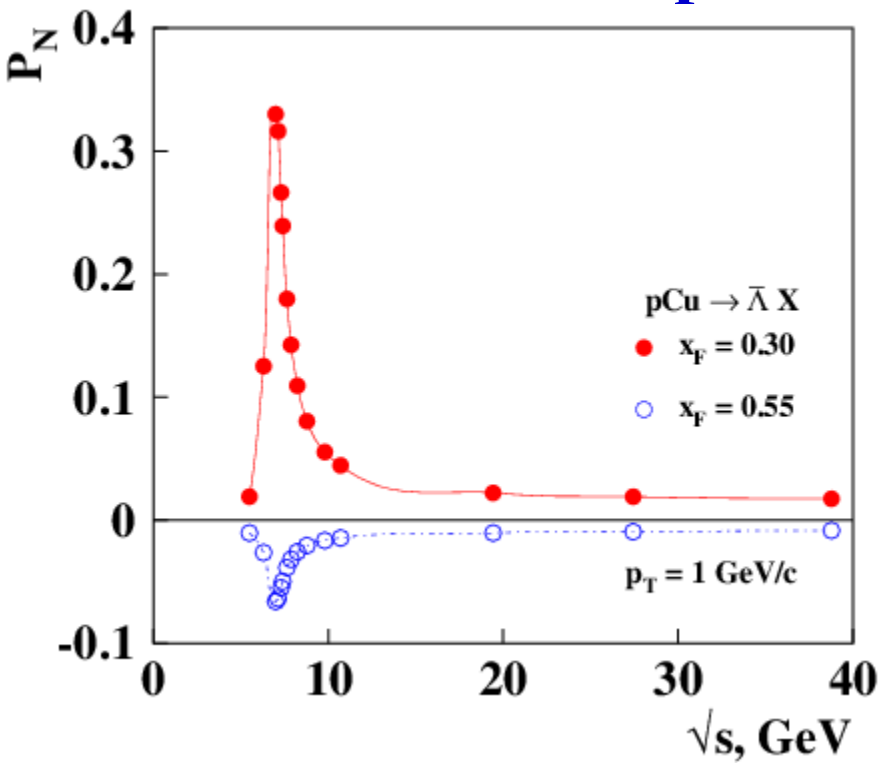

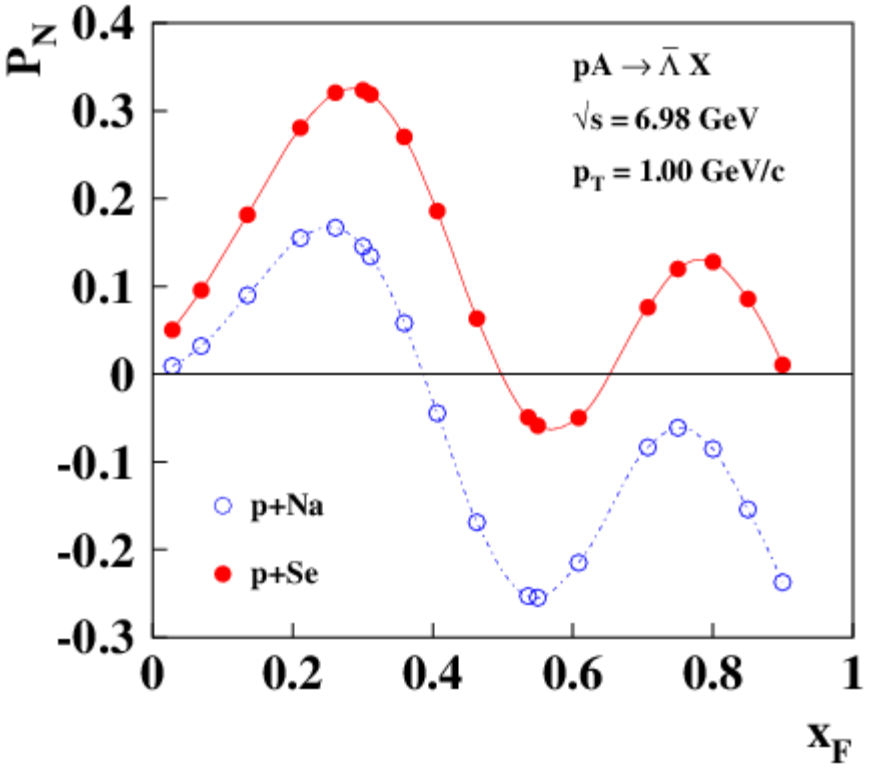

Calculations of $P_N(x_F)$ for the reactions p + A → $\tilde{\Lambda}$ + X are shown above for p_T = 1 GeV / c. "Resonant" dependences $P_N(\sqrt{s})$ and "oscillations" $P_N(x_F)$ are expected. The peak in the $P_N(\sqrt{s})$ dependence is narrow, since only the s̃ quark carries spin in $\tilde{\Lambda}$. To detect oscillations in $P_N(x_F)$, measurements must be taken over a wide x_F range. “Resonance” in $P_N(\sqrt{s})$ and “oscillation" in $P_N(x_F)$ also occur in pp, pd, dd, C + C and Ca + Ca collisions.

Polarization predictions for $A + A \rightarrow \Lambda^{\uparrow} + X$

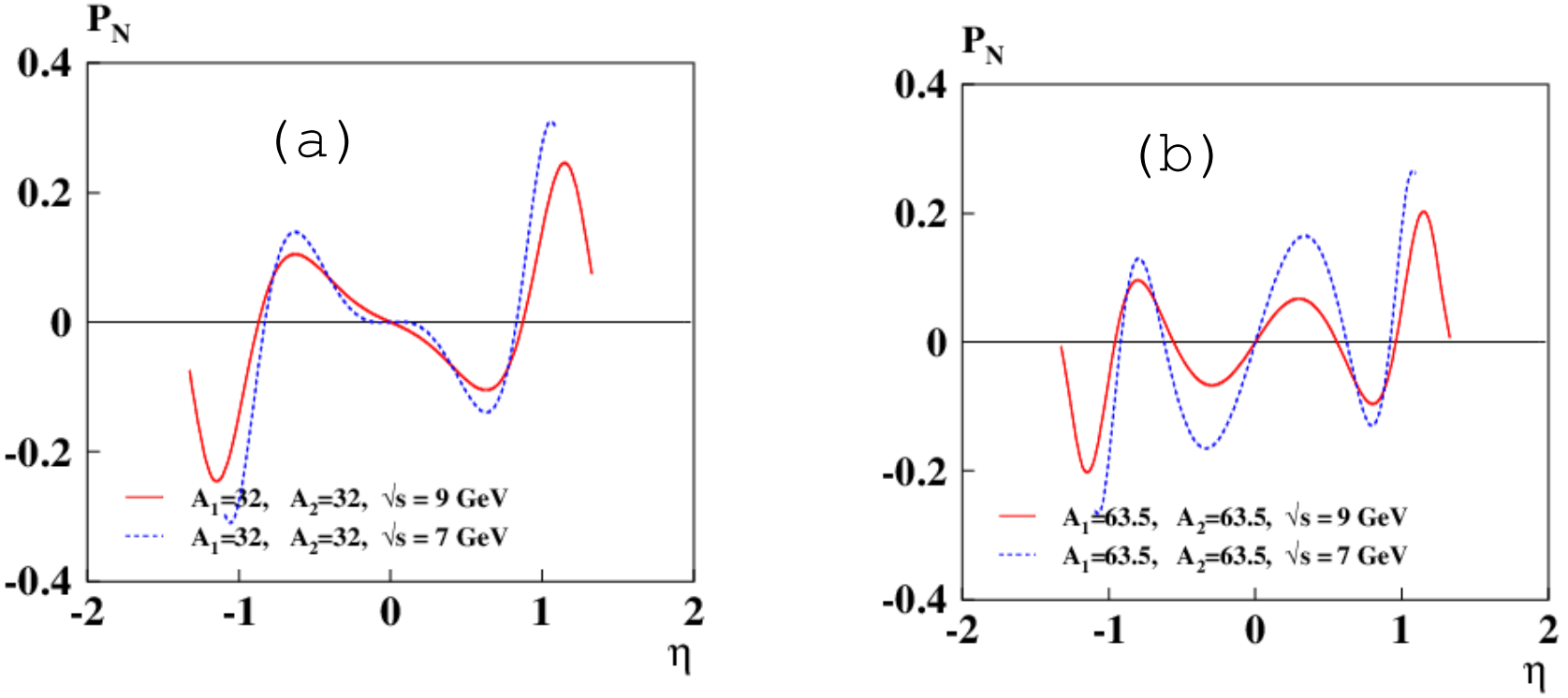

The transverse polarization of vs $\eta = -\ln(\tan(\theta_{cm}/2))$ at $p_T = 2.35$ GeV/c in (a) S+S, (b) Cu+Cu collisions. Solid line corresponds to $\sqrt{s} = 9$ GeV and dashed line to $\sqrt{s} = 7$ GeV, respectively [11]. The higher is the atomic weight of the ions, the higher is the frequency of the oscillations, since the effective chromomagnetic field is increased by the spectator quarks, coming from colliding ions. This effect can be checked at SPD in pp, pd, dd, C + C and Ca + Ca collisions.

Event multiplicity (N_{ch}) dependence of A_N and P_N

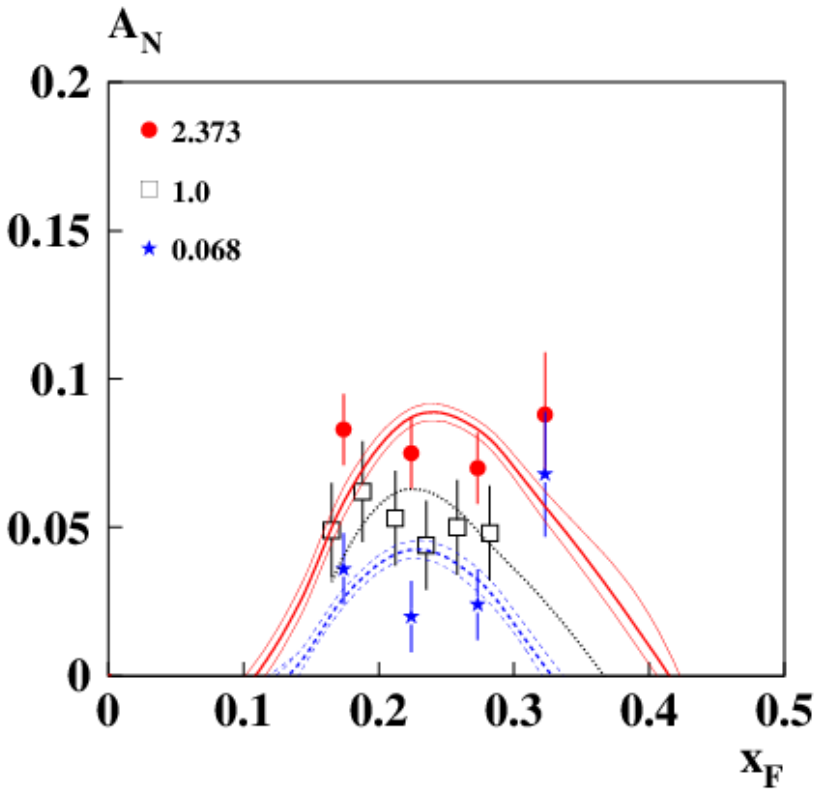

Dependence $A_N(x_F)$ for the $p^{\uparrow} + p \rightarrow \pi^+ + X$ reaction at energy $\sqrt{s}$ = 200 GeV (BRAHMS Collab.). The data and calculated curves were obtained for the ratio of multiplicity to its mean value of 2.373, 1 and 0.068, respectively, as indicated in the figure. In the CPQ model, events with a multiplicity above the mean correspond to diagrams with additional q-$\tilde{q}$ pairs. N_{ch} dependence is expected for A_N and P_N.

Conclusions and outlook

The study of single-spin polarization phenomena in the SPD NICA project makes it possible to reveal the regularities in the behavior of the single-spin asymmetry of hadrons and the transverse polarization of hyperons and antihyperons.
Among the most interesting tasks are the following:

1) Investigation of the phenomenon of A_N and P_N oscillations and the relationship of the oscillation frequency with the number of quarks in a hadron and the type of hadrons participating in the reaction. High oscillation frequency is expected also in heavy ion collisions.

2)Investigation of the threshold phenomena for A_N, including the measurement of the threshold angle of hadron production in the c.m.

3) Investigation of the scaling phenomenon for A_N and P_N and corrections to it, reflecting the peculiarities of the mechanism of the origin of polarization phenomena.

4) Investigation of the phenomenon of "resonance" dependence of A_N and P_N on energy $\sqrt{s}$. Disclosure of the mechanism of this phenomenon.

Conclusions and outlook

5) Investigation the role of color factors for A_N and P_N.

6) Additional possibilities for studying the mechanism of polarization phenomena are provided by the use of such variables as the multiplicity of charged particles in an event, as well as the centrality of collisions and the impact parameter in the case of collisions of nuclei.

The data obtained in the proposed studies will significantly expand the general world database on polarization measurements and become the basis for their systematic theoretical analysis, within the framework of a unified approach. One of the models that makes it possible to carry out a systematic global analysis of polarization data is the model of chromomagnetic polarization of quarks (CPQ), which makes it possible to analyze various reactions in a wide range of kinematic and other variables that determine the experimental conditions.

To obtain a reliable estimate of the measurement error, a complete simulation of the investigated reaction and detector response is required.

Thank you for attention!

References

[1] Abramov V.V. Phenomenology of single-spin effects in hadron production at high energies // Phys. Atom. Nucl. — 2009. — V. 72, no. 11. — P. 1872–1888.
[2] Meshkov I.N. Luminosity of an Ion Collider // Phys. Part. Nucl. — 2019. — V. 50, no. 6. — P. 663–682.

[3] Abramov V.V. A new scaling law for analyzing power in hadron production by transversely polarized baryons // Eur. Phys. J. — 2000. — V. C14 — P. 427–441. — arXiv:0110152 [hep-ph].

[4] Abramov V.V. Universal scaling behavior of the transverse polarization for inclusively produced hyperons in hadron hadron collisions — IHEP 2001-13, 2001. — arXiv:0111128 [hep-ph].

[5] Bonner B.E. et al. Spin Parameter Measurements in and K_S Production // Phys. Rev. — 1988. — V. D38 — P. 729–741.
[6] Bravar A. et al. Analyzing power measurement in inclusive Lambda0 production with a 200-GeV/c polarized proton beam // Phys. Rev. Lett. — 1995. — V. 75 — P. 3073–3077.
[7] Baranov S.P. On the production of doubly flavored baryons in p p, e p and gamma gamma collisions // Phys. Rev. — 1996. — V. D54 — P. 3228–3236.

References

[8] Abramov V.V. Nuclear Effects in the Polarization Phenomena // Proc. of XV Advanced Research Workshop on High Energy Spin Physics (DSPIN-13), Dubna, Oct. 8-12, 2013. — Dubna: JINR. — 423p. 2014. — Ed. by A.V. Efremov and S.V. Goloskokov. — P. 17–20.

[9] Abramov V.V. On the dependence of the single-spin asymmetry of charged pions on kinematical variables// Phys. Atom. Nucl. – 2007. – V. 70, no.12. – P. 2103-2112.

[10] Abramov V.V. Single spin effects in collisions of hadrons and heavy ions at high energy // Proc. of XII Advanced Research Workshop on High Energy Spin Physics (DSPIN-07), Dubna, Sept. 3-7, 2007. — Dubna: JINR. — 454p. 2008. — Ed. by A.V. Efremov and S.V. Goloskokov. – P. 13–16. – arXiv:0711.0323 [hep-ph].

[11] Abramov V.V. Microscopic Stern-Gerlach Effect and Thomas Spin Precession as an Origin of the SSA // Proc. of XIII Advanced Research Workshop on High Energy Spin Physics (DSPIN-09), Dubna, Sept. 1-5, 2009. — Dubna: JINR. — 467p. 2009. — Ed. by A.V. Efremov and S.V. Goloskokov. — P. 25–28. — arXiv:0910.1216 [hep-ph].

[12] Abramov V.V. Single-spin physics: Experimental trends and their origin // J. Phys. Conf. Ser. — 2011. — V. 295. — P. 012086.

References

[13] Abramov V.V. An explanation of the new polarization data in the framework of effective color field model // Proc. of XIV Advanced ResearchWorkshop on High Energy Spin Physics (DSPIN-11), Dubna, Sept. 20-24, 2011. — Dubna: JINR. — 412p. 2012. — Ed. by A.V. Efremov and S.V. Goloskokov. — P. 21–26.

[14] Abramov V.V. Polarization phenomena in hadronic reactions//Phys. Part. Nucl. — 2014. — V. 45, no. 1. —P. 62–65.

[15] Abramov V.V. Single-spin asymmetry in pp and pA-collisions // J. Phys. Conf. Ser. — 2016. — V. 678. — P. 012039.

[16] Abramov V.V. On the A-dependence of the neutron single-spin asymmetry in pA-collisions // J. Phys. Conf. Ser. — 2017. — V. 938. — P. 012038.

[17] Abramov V.V. Polarization of cascade hyperons and antihyperons // J. Phys. Conf. Ser. — 2020. — V. 1435. — P. 012001.

[18] Abramov V.V., Volkov A.A., Goncharov P.I., Kalinin A.Yu., Korablev A.V., Korneev Yu.P., Kostritsky A.V., Krinitsyn A.N., Kryshkin V.I., Markov A.A., Talov V.V., Turchanovich L.K. and Khmelnikov
A.V. Single-spin asymmetry for charged hadrons produced in proton nucleus collisions at 40-GeV for c.m. production angles in the range 40-degrees to 79-degrees // Phys. Atom. Nucl. — 2007. — V. 70, no. 9. — P. 1515–1526.

References

[19] Aidala C. et al. Nuclear Dependence of the Transverse-Single-Spin Asymmetry for Forward Neutron Production in Polarized p+A Collisions at psNN = 200 GeV // Phys. Rev. Lett. — 2018. — V. 120 — P. 022001.
[20] Lee J.H. et al. Cross-sections and Single Spin Asymmetries of Identified Hadrons in p " +p at ps = 200- GeV — 2009. — arXiv:0908.4551 [hep-ex].

[21] Ho P.M. et al. Production polarization and magnetic moment of anti-XI+ anti-hyperons produced by 800- GeV/c protons // Phys. Rev. Lett. — 1990. — V. 65 — P. 1713–1716.
[22] Abouzaid E. et al. 0 and ¯0 Polarization Measurements at 800-GeV/c // Phys. Rev. –– 2007. — V. D75 — P. 012005-1–012005-5.

[23] Felix J. (E766 Collab.) Inclusive ¯ polarization in pp collisions at 27.5 GeV // Proc. of Adriatico Research Conference on Trends in Collider Spin Physics, Trieste, 5-8 Dec. 1995. — Singapore, River Edge, N.J.: World Scientific, 1997. — 1997. — Ed. by Y. Onel, N.Paver, A.Penzo. — P. 231–234.

[24] Bellwied R. for the E896 Collab. The measurement of transverse polarization of Lambda hyperons in relativistic heavy ion collisions // Nucl. Phys. — 2002. — V. A698 –– P. 499c–502c.

BACKUP SLIDES

Quark spin precession in the color field

$d\xi/dt \approx a[\xi\, \mathbf{B}^a]$ (F-T-BMT-equation) (4)

$a = g_s(g^a_Q - 2 + 2M_Q/E_Q)/2M_Q$ (5)

Quark masses $M_U \approx M_D \approx 0.3$ GeV, E_Q – quark energy in c.m.

$\Delta\mu^a_Q = (g^a_Q - 2)/2$ (quark anomalous chromomagnetic moment).

➢Due to the spontaneous breaking of chiral symmetry appear the $\Delta M_Q(q) \approx 0.3$ GeV and $\Delta\mu^a_Q(q)$ of the constituent quarks.

In the instanton model: $\Delta\mu^a_Q(0) \approx -0.4$ **(N. Kochelev);**

$\Delta\mu^a_Q(0) \approx -1.6$ **(D. Diakonov).**

➢Model-dependent (CPQ) estimate of $\Delta\mu^a_Q$ for u,d,s,c,b-quarks are obtained from the global analysis of polarization data:

➢ $\Delta\mu^a_Q$ (u,c) **= -0.4839±0.0017,** q=+2/3;

➢ $\Delta\mu^a_Q$ (d,s,b) ≈ $\sqrt{(2/3)}\,\Delta\mu^a_Q$**(u,c),** q=-1/3.

Quark counting rules for ν_A (A + B → C + X)

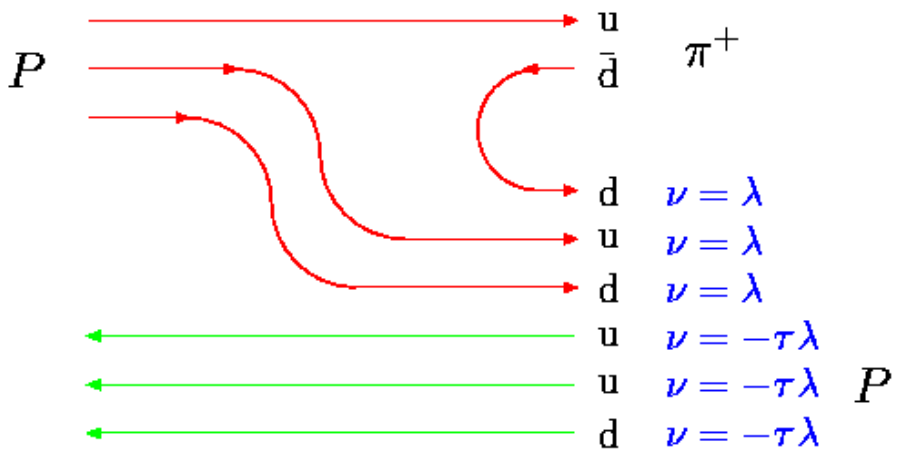

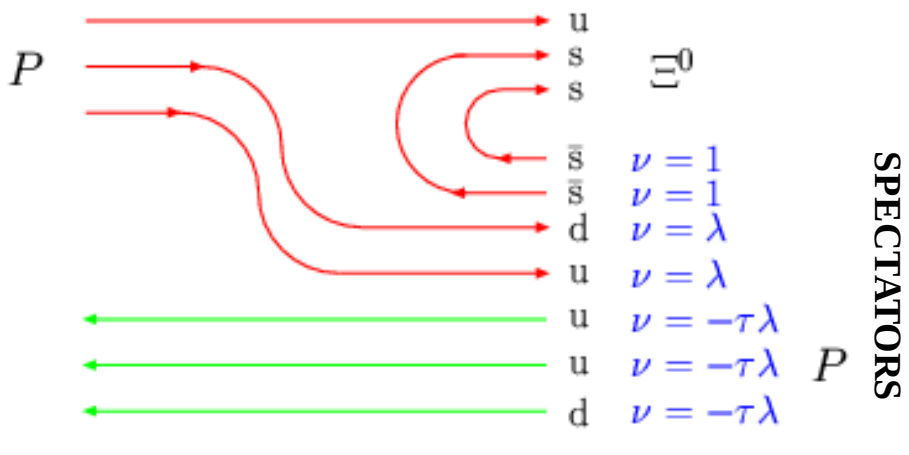

$\int \mathbf{E^a} \sim \int \mathbf{B^a} \sim \nu_A = [3\lambda - 3\tau\lambda] < 0$; $\int \mathbf{E^a} \sim \int \mathbf{B^a} \sim \nu_A = [2 + 2\lambda - 3\tau\lambda] > 0$

$\mathbf{A_N \sim P_U \nu_A (g^a_U - 2)/2M_U > 0;}$ $\mathbf{P_N \sim \nu_A (g^a_S - 2)/2M_S < 0.}$

qq, q̃q̃ -SU(3)$_c$ antitriplet, weight $\nu = \lambda$; $C_F = 2/3$ – color factor

qq̃, q̃q -SU(3)$_c$ singlet, weight $\nu = 1$. $C_F = 4/3$ – color factor

- S.P. Baranov, Phys. Rev. D54, 3228 (1996). $|\psi|^2 \sim (C_F\alpha_S)^3$. (16)
- $\lambda = -|\psi_{qq}(0)|^2 / |\psi_{q\tilde{q}}(0)|^2 \approx 1 - e^{1/8} \approx -0.1332$ **color factor** (17)
- $\lambda = -0.1363 \pm 0.0003$, $\tau = 0.0267 \pm 0.0012$, **fit for 85 reactions.**

Model parameters (global and local)

1) $m_s = 98 \pm 2$ MeV; 2) $m_c = 1264 \pm 17$ MeV; 3) $\Delta\mu^a_u = -0.4839 \pm 0.0017$;

4) $\Delta M_u = 0.2665 \pm 0.0012$; 5) $\Delta M_d = 0.3033 \pm 0.0013$; 6) $\Delta M_s = 0.3703 \pm 0.0020$;

7) $\tau = 0.0267 \pm 0.0005$; 8) $\lambda = -0.1363 \pm 0.0003$; 9) $\varepsilon = -0.00497 \pm 0.00009$;

10) $W_0 = 275.6 \pm 1.3$ GeV; 11) $P_N = 84.7 \pm 0.4$ GeV; 12) $m_r = 0.3573 \pm 0.0016$ GeV;

13) $n_q = 4.671 \pm 0.018$; 14) $A_a = 10.35 \pm 0.55$; 15) $A_b = 0.3084 \pm 0.0012$;

16) $A_T = 59.6 \pm 5.8$; 17) $\delta_R = 0.2907 \pm 0.0026$; 18) $a_f = 3.092 \pm 0.047$;

19) $V_T = 0.1437 \pm 0.062$; 20) $p_m = 0.152 \pm 0.038$ GeV; 21) $a_{81} = 1.622 \pm 0.050$;

22) $a_{56} = 0.4220 \pm 0.0013$ GeV; 23) $E_0 = -83.8 \pm 0.4$ GeV; 23) $a_{51} = 0.0236 \pm 0.0015$;

25) $E_c = 0.000511 \pm 0.000003$; 26) $a_{41} = 0.1428 \pm 0.0013$; 27) $\eta = -1.761 \pm 1.18$;

$W_0 \approx m_p^2/m_q \approx 255 \pm 24$ GeV; $m_q \approx (m_u + m_d)/2 \approx 3.45 \pm 0.33$MeV; $\lambda \approx 1 - \exp(1/8) \approx -0.133$;

Global Data Analysis: A_N

Inclusive reactions, in which was measured single-spin asymmetry in hadron-hadron collisions (26 reactions).

№	Reaction	№	Reaction	№	Reaction
1	$p^{\uparrow}\, p(A) \rightarrow \pi^{+}$	10	$p^{\uparrow}\, A \rightarrow J/\psi^{\uparrow}$	19	$\pi^{+}\, p^{\uparrow} \rightarrow \pi^{+}$
2	$p^{\uparrow}\, p(A) \rightarrow \pi^{-}$	11	$p^{\uparrow}\, p \rightarrow \eta$	20	$\pi^{-}\, p^{\uparrow} \rightarrow \pi^{-}$
3	$p^{\uparrow}\, p \rightarrow \pi^{0}$	12	$d^{\uparrow}\, A \rightarrow \pi^{+}$	21	$\pi^{-}\, p^{\uparrow} \rightarrow \pi^{0}$
4	$p^{\uparrow}\, p(A) \rightarrow K^{+}$	13	$d^{\uparrow}\, A \rightarrow \pi^{-}$	22	$\pi^{-}\, d^{\uparrow} \rightarrow \pi^{0}$
5	$p^{\uparrow}\, p(A) \rightarrow K^{-}$	14	$\tilde{p}^{\uparrow}\, p \rightarrow \pi^{+}$	23	$K^{-}\, d^{\uparrow} \rightarrow \pi^{0}$
6	$p^{\uparrow}\, p \rightarrow K^{0}_{S}$	15	$\tilde{p}^{\uparrow}\, p \rightarrow \pi^{-}$	24	$K^{-}\, p^{\uparrow} \rightarrow \pi^{0}$
7	$p^{\uparrow}\, p(A) \rightarrow n$	16	$\tilde{p}^{\uparrow}\, p \rightarrow \pi^{0}$	25	$\pi^{-}\, p^{\uparrow} \rightarrow \eta$
8	$p^{\uparrow}\, p(A) \rightarrow p$	17	$\tilde{p}^{\uparrow}\, p \rightarrow \eta$	26	$\tilde{p}\, p^{\uparrow} \rightarrow \pi^{0}$
9	$p^{\uparrow}\, A \rightarrow \tilde{p}$	18	$\tilde{p}\, d^{\uparrow} \rightarrow \pi^{0}$		

Global Data Analysis: P_N

Inclusive reactions, in which was measured hyperon polarization in hadron-hadron collisions (31 reactions).

№	Reaction	№	Reaction	№	Reaction
27	$p\,p(A) \to \Lambda^{\uparrow}$	37	$\Sigma^{-}\,A \to \Sigma^{+\uparrow}$	48	$K^{-}\,p \to \Lambda^{\uparrow}$
28	$p\,A \to \Xi^{-\uparrow}$	38	$\Sigma^{-}\,A \to \Xi^{-\uparrow}$	49	$K^{-}\,A \to \Xi^{-\uparrow}$
29	$p\,A \to \Xi^{0\uparrow}$	39	$p\,A \to \tilde{\Lambda}^{\uparrow}$	50	$\pi^{-}\,A \to \Xi^{-\uparrow}$
30	$p\,A \to \Sigma^{+\uparrow}$	40	$\Sigma^{-}\,A \to \tilde{\Lambda}^{\uparrow}$	51	$\pi^{+}\,p \to \Lambda^{\uparrow}$
31	$p\,p \to p^{\uparrow}$	41	$p\,A \to \tilde{\Xi}^{+\uparrow}$	52	$K^{+}\,p \to \Lambda^{\uparrow}$
32	$p\,A \to \Sigma^{-\uparrow}$	42	$p\,A \to \tilde{\Xi}^{0\uparrow}$	53	$\pi^{-}\,p \to \Lambda^{\uparrow}$
33	$p\,A \to \Omega^{-\uparrow}$	43	$p\,A \to \tilde{\Sigma}^{-\uparrow}$	54	$K^{+}\,p \to \tilde{\Lambda}^{\uparrow}$
34	$\Sigma^{-}\,A \to \Lambda^{\uparrow}$	44	$\tilde{p}\,A \to \tilde{\Lambda}^{\uparrow}$	55	$\pi^{-}\,p \to \tilde{\Lambda}^{\uparrow}$
35	$p\,A \to \Sigma^{0\uparrow}$	45	$A_1+A_2 \to \Lambda^{\uparrow}$	56	$K^{-}\,p \to \tilde{\Lambda}^{\uparrow}$
36	$\Lambda\,A \to \Omega^{-\uparrow}$	46	$Au+Au \to \Lambda^{\uparrow(Glob)}$	57	$\pi^{-}\,A \to \tilde{\Xi}^{+\uparrow}$
		47	$Au+Au \to \tilde{\Lambda}^{\uparrow(GloB)}$		

Global Data Analysis: A_N, P_N, ρ_{00}

Other inclusive reactions, in which was measured vector meson polarization and lepton induced reactions (24 reactions).

№	Reaction	№	Reaction	№	Reaction
58	$p\,A \to J/\psi^{\uparrow}$	67	$n\,A \to K^*(892)^{-\uparrow}$	73	$e^+\,A \to \Lambda^{\uparrow}$
59	$\tilde{p}\,A \to J/\psi^{\uparrow}$	68	$n\,A \to K^*(892)^{+\uparrow}$	74	$e^+\,A \to \tilde{\Lambda}^{\uparrow}$
60	$p\,A \to Y(1S)^{\uparrow}$	69	$p\,p \to \varphi(1020)^{\uparrow}$	75	$e^+\,p^{\uparrow} \to \pi^+$
61	$p\,A \to Y(2S)^{\uparrow}$	70	$\tilde{p}\,p \to \rho(770)^{\uparrow}$	76	$e^+\,p^{\uparrow} \to \pi^-$
62	$p\,p \to Y(1S)^{\uparrow(\tilde{\lambda})}$	71	$AuAu \to \tilde{K}^*(892)^{0\uparrow}$	77	$e^+\,p^{\uparrow} \to K^+$
63	$p\,p \to Y(2S)^{\uparrow(\tilde{\lambda})}$	72	$AuAu \to \varphi(1020)^{\uparrow}$	78	$e^+\,p^{\uparrow} \to K^-$
64	$p\,p \to Y(3S)^{\uparrow(\tilde{\lambda})}$			79	$\mu^-\,6LiD^{\uparrow} \to h^+$
65	$\tilde{p}\,p \to Y(1S)^{\uparrow}$			80	$\mu^-\,6LiD^{\uparrow} \to h^-$
66	$\tilde{p}\,p \to Y(2S)^{\uparrow}$			81	$\nu_\mu\,A \to \Lambda^{\uparrow}$